Inhibition-Produced Patterning in Chains of Coupled Nonlinear Oscillators

G. B. Ermentrout, N. Kopell

SIAM Journal on Applied Mathematics, Volume 54, Issue 2 (Apr., 1994), 478-507.

SIAM J. APPL. MATH.
Vol. 54, No. 2, pp. 478–507, April 1994

010

INHIBITION-PRODUCED PATTERNING IN CHAINS OF COUPLED NONLINEAR OSCILLATORS*

G. B. ERMENTROUT† AND N. KOPELL‡

Abstract. This paper describes the behavior of chains of oscillators in which there is both local coupling and coupling between points on the chain that are roughly a distance of a half-chain apart. The local coupling is designed to produce synchrony, while the long-distance coupling is an abstraction of inhibitory coupling: alone it would produce antiphase behavior between the oscillators directly coupled. The investigation is motivated by data concerning traveling waves of electrical activity in the nervous system of animals that swim in an undulatory manner and also by observations concerning the motor behavior of more general vertebrates in early development. The aim of the work is to show that this connectivity can give rise to waves with wavelength equal to the length of the chain, as observed in swimming animals, as well as the more complicated patterns seen in early development. The latter include "S-waves," in which the two halves of the chain are each in synchrony but are oscillating in antiphase with one another. It is shown that there are families of stable solutions, including traveling waves with several wavelengths within the chain, and "antiwaves" with a leading or lagging oscillator near the center of the chain. Several qualitatively different solutions can be stable for the same parameter values. Changing the connectivity of the long-range coupling can alter the repertoire of possible behaviors.

Key words. nonlinear oscillator, pattern formation, inhibition, central pattern generator, development

AMS subject classifications. 92C15, 92C20

1. Introduction. This paper was inspired by questions arising from central pattern generators (CPGs), which are networks of neurons that govern rhythmic motor output. One such CPG that has been intensively studied is the network that produces and regulates undulatory locomotion in fish-like animals, notably the lamprey [1]–[3]. The isolated spinal cord of a lamprey, which contains the CPG, is capable of spontaneously self-organizing into spatio-temporal patterns of electrical activity that are essentially the same as in an intact, behaving animal [4]. These patterns are roughly constant-speed traveling waves. The waves retain their wavelength under change of swimming speed, a wavelength that is approximately the body length of the animal. Furthermore, there is a consensus that the CPG may be described as a linear array of oscillators [5], [6]. In previous papers [7], [8] it was shown that such constant-speed traveling waves are possible, even generic, for a linear array of limit cycle oscillators coupled locally by nearest-neighbor or multiple-neighbor connections. (See [7]–[9] for the technical hypotheses, including the validity of the use of the averaging method.) This work suggested mechanisms for the regulation of wavelength with changing swimming speed, but did not suggest any reason why the wavelength is related to body length. Indeed, for nearest-neighbor or other types of local coupling, there is no intrinsic wavelength; the coupling specifies the phase lag between succes-

*Received by the editors May 29, 1992; accepted for publication (in revised form) May 27, 1993.
†Department of Mathematics and Statistics, University of Pittsburgh, Pittsburgh, Pennsylvania 15260. The work of this author was supported in part by National Science Foundation grant DMS-9002028.
‡Department of Mathematics, Boston University, Boston, Massachusetts 02215. The work of this author was supported in part by National Science Foundation grant DMS-9200131 and National Institute of Mental Health grant NIMH-47150.

sive oscillators in the chain, rather than the lag between the two ends, which grows with the length of the chain.

The main purpose of the paper is to explore possibilities for the origin of the experimentally observed wavelength. Although many observations on the behavior of the lamprey cord have been explained using only local coupling [1], [10], [11], it is known that there are direct connections between cells at a distance apart that is a significant fraction of the total length of the cord [12], [13]. In this paper, we continue to consider the network as a chain of limit cycle oscillators; we now consider the effects of adding to the local coupling between oscillators long-range connections that extend to or slightly beyond half the length of the chain. As in previous papers [5], [7], [8], [14], [15], we work with phase oscillators whose interactions are via the differences of the phases. (See [16] for a discussion of when more general oscillators and interactions can be so described without loss of generality.)

The long-range connections that we use have different properties than the local connections. The local connections are chosen so that, in the absence of the long-range connections, the oscillators in the chain are in synchrony. By contrast, the long-range coupling is chosen so that there is a stable phase difference of π for the oscillators directly coupled. As discussed in [17], models of neural oscillators coupled using models of fast (relative to the period of the oscillator) inhibitory synapses have such stable antiphase solutions. In this sense, the long-range coupling provides an abstract version of inhibition. The choice of local coupling that is synchronizing comes from the second main biological motivation, involving early development in vertebrates, to be discussed below.

We wish to show how the presence of such long-range inhibition can induce patterning in a chain of oscillators whose local connections alone would induce synchrony. The ideas are related to notions of lateral inhibition, which is believed to be important in many patterned phenomena (e.g., animal coat makings, hallucination patterns, occular dominance stripes [18]). Those patterns have been the subject of intense mathematical effort (see references in [18] and [19]). In that body of work, pioneered by Turing [20], the equations describing the local dynamics have a stable critical point, and the inhibition acts to destabilize the spatially homogeneous solution. This work does not give direct information about the behavior of oscillators in the presence of long-range inhibition. An early investigation into the effects of long-range coupling in a chain of oscillators was done by Kiemel [14], who found unexpected patterns when long-range coupling in one direction was added to local coupling that is not symmetric in the two directions. In [21] Ermentrout described the effects of long-range coupling on the stability of the synchronized state in a *ring* of oscillators. Such a circular geometry lacks edge effects that produce patterning in a linear geometry [7].

The choice of connectivity for the long-range coupling was influenced by observations about early development in vertebrates [22]. In many observed vertebrate species, there is a sequence of behavioral changes that happens in the very early stages of development, during which the gross morphology of the animal is tadpole-like [22], [23]. An early set of motions involves bending of the head, without regular motion of the rest of the body. This is followed by a stage of movements known as "C-coils," in which the muscles along one side of the body contract simultaneously, creating a C-shaped flexion. These C-coils can be rhythmic, with the flexion occurring alternately to the two sides. In a somewhat later stage of development, in animals that ultimately locomote in an undulatory manner, the C-coils are replaced by traveling

waves of flexion that are reminiscent of the traveling waves associated with adult locomotion. In animals such as salamanders, we see instead an alternating gate of limbs in which the movements of the spine appear to be what is known as an "S-wave": The front section of the body exhibits simultaneous contractions, producing a flexion to one side, while the back section of the body contracts in unison to produce a flexion to the other side; thus the front and back halves produce rhythmic movements in antiphase with each other. The shape produced in the animal is that of an S, with a node between the two halves. Between the rhythmic C-coils and the more advanced behavior, there is sometimes observed motion that has been described as S-waves and traveling waves, with waves superimposed on a pattern that seems to have a node [23].

In this paper, we show how long-range connections between oscillators at the ends of the chain and oscillators near the middle of the chain can produce patterns similar to those observed in early development and can produce stable traveling waves with the observed wavelength. We also show that several qualitatively different solutions may be stable for the same parameter values and that changing some details of the connectivity can change the possible repertoire of qualitative behavior. In addition, we show that, in some circumstances, patterns that exist stably for short chains cannot exist stably for much longer ones and we give numerical evidence to show that chains with multiple neighbor local connections behave like chains containing many fewer oscillators.

The equations we investigate have the general form

$$\theta_j' = \omega_j + \sum_{k=1}^{N} h_{kj}(\theta_k - \theta_j). \tag{1.1}$$

By local coupling, we mean $k = j \pm 1$. This coupling satisfies $h_{kj}(0) = 0$ and $h'_{kj}(0) > 0$. As we show in §2, with this coupling alone and $\omega_j \equiv w$, the synchronous solution $\theta_j \equiv \theta_k$ exists and is stable (see also [5]). The long-range coupling functions h_{kj} satisfy $h_{kj}(\pi) = 0$, $h'_{kj}(\pi) > 0$; in the absence of other coupling, it would produce a stable antiphase solution between the jth and kth oscillators.

We are interested in the existence and stability of solutions that are qualitatively like those described above, i.e., traveling waves and S-waves. In addition, we introduce a type of solution we call "antiwaves" (corresponding to a pair of approximate traveling waves going toward or away from the center of the chain). Even with simple choices for the functions h_{kj} and sparse connectivity for the long-range connections, we have not found it possible to obtain complete results. We present here analyses of the behavior in various asymptotic limits. In particular, for each of several cases with fixed connectivity among the oscillators, we vary the strengths of the long-range interactions (i.e., the amplitudes of the functions h_{kj}, $k \neq j \pm 1$). The long-range interactions are divided into "inward," from the edges of the chain to oscillators near the middle of the chain, and "outward," in which oscillators near the middle affect the ones at the ends. Most of the analytic results are for asymptotic regimes in which one or both kinds of long-range coupling are strong relative to the local coupling, or the chain is very long. We have supplemented these analytical results by numerical simulations to arrive at our conjectured picture of the possible types of behavior with time-independent phase differences. We also include parameter regimes in which there is more complicated time-dependent behavior.

The main results of the paper are in §2, which discusses chains with long, isolated connections that extend slightly beyond half the length of the chain (see Fig. 1(a)). We

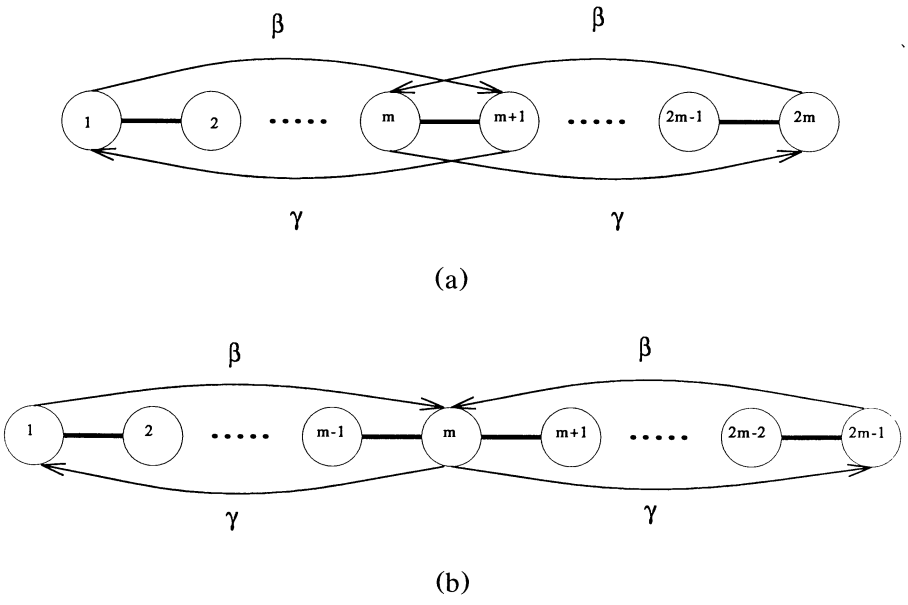

FIG. 1. *Chains of oscillators with half-length inhibitory fibers* (a) *overlap topology* (b) *one-point inhibition.*

find that inward and outward long coupling result in different sets of stable solutions. With inward coupling alone, we find (for various coupling sizes) synchrony, S-waves, antiwaves, or combinations of them. Stable traveling waves require some outward coupling. In contrast, S-waves are stabilized by large values of inward coupling and destabilized by large values of outward coupling. Antiwaves can coexist stably with traveling waves or S-waves. Long chains can produce a large number of qualitatively different patterns, among them traveling waves of many different wavelengths, including the one whose wavelength is the length of the chain, and the bifurcation diagram is very complicated. In such long chains, synchrony is destabilized by small amounts of inward or outward coupling. The stability analyses are made possible by a result [24] that yields stability whenever certain simple inequalities hold on the phase lags. We also consider "half-chains," with inhibition directly between the two ends of the chain instead of between two ends and the middle; a special case of this was analyzed in [5]. The analysis follows from that of one-half of the chain coupled using long connections to slightly beyond half the length of the chain.

The results of §2 are achieved by exploiting special (and nongeneric) symmetry properties in the choice of the functions $\{h_{kj}\}$ and the connectivity. For finite chains, the stability results imply robustness under perturbation, which shows that the symmetry properties are not necessary for the results we describe. However, the allowable perturbations could go to zero as the chain grows. In §3 we investigate the effect on the solutions of variations in the equations that retain the connectivity used in the previous section. One result from asymptotic analysis is that, if the local coupling is not symmetric in the two directions, antiwave solutions are not possible for long enough chains. We also describe numerical simulations used to explore the effect of other changes.

In §4 we consider the behavior of chains in which the long connections are between the end oscillators and a *single* oscillator at the center of the chain (Fig. 1(b)). We find a behavioral repertoire for such chains that is a subset of that discussed in §2 with the S-waves absent. The analysis is much simpler and yields results similar to those of §2, at least for large outward coupling. In §5 we use numerics to look at the effects of translation-invariant connections between distant points, allowing the strengths in the two directions to be different.

In §6 we discuss aspects of the relationship between the motivating data described above and the mathematical results. We also discuss a further mathematical issue concerning scaling effects of chain size in the presence of multiple-neighbor coupling.

2. Chains with half-length fibers and overlap. To obtain sharp analytical results, we use possible symmetries and choose $N = 2m$. The connections we investigate then extend between oscillator 1 and oscillator $m+1$ and between oscillator m and oscillator $2m$, as in Fig. 1(a). (As we argue and show numerically, the qualitative behavior persists when the symmetries are removed.) The equations are then special cases of (1.1), with $h_{kj} = 0$ if $k \neq j+1$ or $j-1$, unless $j = 1, m, m+1, 2m$. Thus, for $j \neq 1$, m, $m+1$, or $2m$, the equations have the form

$$(2.1)_j \qquad \frac{d\theta_j}{dt} = \omega + h^+(\theta_{j+1} - \theta_j) + h^-(\theta_{j-1} - \theta_j),$$

where $h^+(\cdot) = h^-(\cdot) = \sin(\cdot) \equiv h(\cdot)$. The remaining equations are

$$(2.1)_1 \qquad \frac{d\theta_1}{dt} = \omega + h^+(\theta_2 - \theta_1) + f^+(\theta_{m+1} - \theta_1),$$

$$(2.1)_{2m} \qquad \frac{d\theta_{2m}}{dt} = \omega + h^-(\theta_{2m-1} - \theta_{2m}) + f^-(\theta_m - \theta_{2m}),$$

$$(2.1)_m \qquad \frac{d\theta_m}{dt} = \omega + h^+(\theta_{m+1} - \theta_m) + h^-(\theta_{m-1} - \theta_m) + g^+(\theta_{2m} - \theta_m),$$

$$(2.1)_{m+1} \qquad \frac{d\theta_{m+1}}{dt} = \omega + h^+(\theta_{m+2} - \theta_{m+1}) + h^-(\theta_m - \theta_{m+1}) + g^-(\theta_1 - \theta_{m+1}).$$

The functions f^+ and f^- specify the outward coupling from the center oscillators to the ends; the functions g^+ and g^- describe the inward coupling. For all our analytic results, we use $f^+(\cdot) = f^-(\cdot) = -\gamma \sin(\cdot) \equiv f(\cdot)$. Similarly, $g^+(\cdot) = g^-(\cdot) = -\beta \sin(\cdot) \equiv g(\cdot)$. Note that these functions have the abstract property of "inhibition" described in §1. The parameters γ and β then represent the strengths of the inhibition of the outward and inward coupling. It is convenient to write (2.1) in terms of the phase differences $\phi_j \equiv \theta_{j+1} - \theta_j$. Equations (2.1) are then

$$(2.2)_j \qquad \frac{d\phi_j}{dt} = h(\phi_{j+1}) - h(\phi_j) + h(-\phi_j) - h(-\phi_{j-1})$$

for $j \neq 1$, $m-1$, m, $m+1$, and $2m-1$. The other equations are

$$(2.2)_1 \qquad \frac{d\phi_1}{dt} = h(\phi_2) - h(\phi_1) + h(-\phi_1) - f\left(\sum_{j=1}^{m} \phi_j\right),$$

$(2.2)_{m-1}$

$$\frac{d\phi_{m-1}}{dt} = h(\phi_m) - h(\phi_{m-1}) + h(-\phi_{m-1}) - h(-\phi_{m-2}) + g\left(\sum_{j=m}^{2m-1} \phi_j\right),$$

$$(2.2)_m \qquad \frac{d\phi_m}{dt} = h(\phi_{m+1}) - h(\phi_m) + h(-\phi_m) - h(-\phi_{m-1}) + g\left(-\sum_{j=1}^{m} \phi_j\right) - g\left(\sum_{j=m}^{2m-1} \phi_j\right),$$

$(2.2)_{m+1}$

$$\frac{d\phi_{m+1}}{dt} = h(\phi_{m+2}) - h(\phi_{m+1}) + h(-\phi_{m+1}) - h(-\phi_m) - g\left(-\sum_{j=1}^{m} \phi_j\right),$$

$(2.2)_{2m-1}$

$$\frac{d\phi_{2m-1}}{dt} = -h(\phi_{2m-1}) + h(-\phi_{2m-1}) - h(-\phi_{2m-2}) + f\left(-\sum_{j=m}^{2m-1} \phi_j\right).$$

In phase-difference variables $\{\phi_j\}$, a phase-locked solution is one in which $d\phi_j/dt$ vanishes identically. For such solutions, there is a common time-independent frequency $\Omega = d\theta_j/dt$.

We are interested in the solutions that behave like the traveling waves and S-waves described in the Introduction. We have also found another class of solutions, the antiwaves, which are candidates for the intermediate behavior described above. For (2.2), we can look for such solutions by introducing an ansatz for each type. Such an ansatz defines more precisely what we mean by each class of solution.

By an S-wave, we mean a solution in which

$$(2.3) \qquad \phi_m = \pi, \qquad \phi_j = 0 \quad \text{for } j \neq m.$$

For solutions (2.3), the oscillators are in synchrony in each half, with the halves in antiphase. By a traveling wave, we mean a solution of the form

$$(2.4) \qquad \phi_m = \xi, \qquad \phi_j \equiv \bar{\phi} \neq 0, \pi \quad \text{for } j \neq m,$$

where ξ and $\bar{\phi}$ are constants. Note that this is slightly more general than the usual notion of traveling wave, for which the phase lags are all equal (i.e., $\bar{\phi} = \xi$). Antiwaves are solutions of the form

$$(2.5) \qquad \phi_j = -\phi_{2m-j}, \qquad \phi_m = 0.$$

For solutions satisfying (2.5), the phase differences are antisymmetric across the middle, and the actual phases θ_j prove to have a local extremum at $j = m$.

To explore the stability of these solutions, it is useful to have a general stability result. The following is a special case of a theorem in [24]. It states that a solution is

stable, provided that the pattern of phase lags is such that all the coupling functions have nonnegative derivatives at the appropriate values of their arguments, and that the local coupling is stabilizing.

THEOREM 2.1 (see [24]). *Let* $\{\bar\theta_j\}$ *be a phase-locked solution to* (2.1) *for some* Ω. *Suppose that the following conditions hold*:

(i) $(h^{\pm})'(\bar\theta_{j\pm1}-\bar\theta_j)\equiv\alpha_j^{\pm}>0$,

(ii) $(f^{+})'(\bar\theta_{m+1}-\bar\theta_1)\equiv\gamma^{+}\geq 0$,

(iii) $(f^{-})'(\bar\theta_m-\bar\theta_N)\equiv\gamma^{-}\geq 0$,

(iv) $(g^{+})'(\bar\theta_N-\bar\theta_m)\equiv\beta^{+}\geq 0$,

(v) $(g^{-})'(\bar\theta_1-\bar\theta_{m+1})\equiv\beta^{-}\geq 0$.

Then the periodic solution is stable; *i.e., there is a simple zero eigenvalue for the linearized equations corresponding to* (2.1), *with all the other eigenvalues in the left-hand plane. Equivalently, the associated time-independent solution to* (2.2) *is asymptotically stable.* □

Remark. The conditions of Theorem 2.1 are not necessary. Indeed, since those conditions imply that the eigenvalues in question have negative real part, conditions (ii) through (v) may be weakened by allowing the derivatives of f and g to be slightly negative.

The following corollary is later applied to understand stability of the traveling waves and antiwaves.

COROLLARY 2.1. *Let* $\{\bar\phi_j\}$ *be a traveling wave or antiwave solution to* (2.2), *with* $h(\phi)=\sin\phi$ *and* $f=g=-\sin\phi$. *A sufficient condition for stability is that* (i) $|\bar\phi_j|<\pi/2$ *and* (ii) $\cos(\sum_{j=1}^{m}\bar\phi_j)<0$.

Proof. Condition (i) of the hypothesis implies condition (i) of Theorem 2.1, and condition (ii) of the hypothesis, plus the symmetry condition of (2.4) or (2.5), implies all the other hypotheses of the theorem. □

For (2.2), the synchronous solution exists for all values of β and γ, as does the S-wave solution. Less apparent are the circumstances under which these are stable, or the nature of the stable solutions that emerge when these lose stability. The traveling wave and antiwave solutions do not exist for all β and γ and are among the solutions that replace the synchronous and S-wave solutions when the latter become unstable. We use different methods to analyze the existence and stability of the different types of solutions, so we discuss each class separately. Then we give a bifurcation diagram (Fig. 2) that combines many of these results, along with numerical results, to provide much of our conjectured picture of the position in β,γ space of stable patterned solutions to (2.2).

Some of the bifurcation results use the coupling strengths β and γ as bifurcation parameters. Hence we start with the case of $\beta=0=\gamma$, i.e., a chain with only local coupling. It is easy to see that there are then 2^{N-1} solutions to (2.2), which are obtained by allowing ϕ_j to be either 0 or π for each $j=1,N-1$. However, as shown in Proposition 2.1, only the synchronous solution is stable.

PROPOSITION 2.1. *Suppose that* $\beta=\gamma=0$ *in* (2.2), *with* $h=\sin\phi$. *Then only the solution* $\phi_j\equiv 0$ *is stable.*

Proof. Consider (2.2) linearized around some solution. Suppose that there is a value of j for which $\phi_j=\pi$. Then the jth diagonal entry $-2h'(\pi)=2$ is positive and equal in magnitude to twice the off-diagonal entries $|h'(0)|=|h'(\pi)|=1$. From the Gershgorin theorem, it follows that one eigenvalue satisfies $|\lambda-2|\leq 2$. Thus, λ must have a nonnegative real part. It was shown in [16, Prop. A1] that matrices of this form have no zero eigenvalues. Thus there is an eigenvalue with positive real part. □

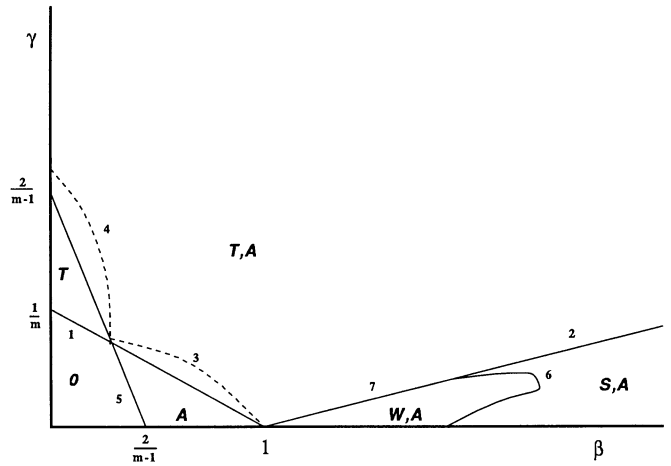

FIG. 2. *Partial bifurcation diagram for chains of oscillators with overlap in long-range connections. The stable antiwave* A, S-*wave* S, *traveling wave* T, *and wobble solutions* W *are marked along with regions of stable synchrony* O. *The numbers in the diagram correspond to the bifurcations described below. Saddle-node bifurcation curves are given in Fig.* 3. (1) *Traveling waves bifurcate from synchronous solutions (pitchfork bifurcation).* (2) S-*waves lose stability at zero eigenvalue and become* T-*waves.* (3) *Unstable traveling waves become stable via secondary bifurcation (numerical).* (4) *Unstable antiwaves become stable via secondary bifurcation (numerical).* (5) *Antiwaves bifurcate from synchrony (pitchfork bifurcation).* (6) *As* β *decreases,* S-*waves go through Hopf bifurcation to become stable "wobbles" (numerical).* (7) *As* β *decreases further, the wobbles die on an infinite period solution.*

Some of the unstable solutions are of interest, since they give rise to stable solutions of the form (2.3), (2.4), or (2.5) as β and/or γ is increased.

Bifurcation, existence, and stability of traveling waves. The traveling wave solutions, described by (2.4), are easier to analyze than the antiwaves because they involve only two unknowns $\bar{\phi}$ and ξ, independent of the length of the chain. From (2.2) and (2.4), these must satisfy

$$-\sin\bar{\phi}+\gamma\sin[(m-1)\bar{\phi}+\xi]=0, \tag{2.6}$$

$$-\sin\bar{\phi}+\sin\xi-\beta\sin[(m-1)\bar{\phi}+\xi]=0.$$

At $\gamma=0$, there are no solutions to (2.6) other than the ones in which $\sin\bar{\phi}=0$. Thus $\gamma>0$ (i.e., inhibition from the middle to the ends) is a necessary condition for the existence of nontrivial traveling waves of the form (2.4). In the next theorem, we show that there are (pitchfork) bifurcations of such solutions off both the synchronous and the S-wave solutions as γ increases; the necessary values of γ goes to zero as the chain grows in size.

In addition to the primary branch of solutions that bifurcate off the $\bar{\phi}=0$ and S-wave solutions (and which appear numerically to tend to waves with wavelength equal to the length of the chains as γ or m increases), there are multiple branches that emerge through saddle-node bifurcations. These curves are known only numerically, except in certain asymptotic regimes, e.g., $\beta\ll 1$ or $\beta,\gamma\gg 1$ with $\beta/\gamma=0(1)$. In those regimes it is possible to obtain not only existence but more qualitative information. In particular, it is possible to see that the latter branches correspond to waves with a larger integral number of wavelengths within the chain, while the former (with $\beta\ll 1$) have a half-integer number of wavelengths. Only those with $\beta\ll 1$ have $\xi\approx\bar{\phi}$, approximating the usual notion of traveling waves in which all phase differences are equal. The bifurcation diagrams of these saddle-node curves, supplemented

by numerics, prove to be very complicated and dependent on whether m is odd or even. Furthermore, the stability of the resulting solutions is not established analytically. The reader interested mainly in the broad picture is advised to omit parts (b) and (c) of Theorem 2.2.

The interpretation of the solutions as waves with higher wavenumber is strengthened by asymptotic analysis of the solutions to (2.6) in the regimes β fixed and m or γ growing without bound. For these solutions, $\xi - \bar{\phi} \to 0$ in the limit, and the solutions have an integral number of wavelengths within the chain in the limit. Neither family of the previous paragraph has both of those properties. Though the proof does not show that these solutions are connected to the bifurcations in the previous paragraph, numerical results suggest that they are, and we comment on our numerical observations. There are roughly $m/2$ such families of traveling waves (plus their mirror images); the general stability result, Theorem 2.1, is used to show that half of these are stable. By contrast, if β is sufficiently large and γ and m are fixed, there are no traveling waves. Comments on further results derived numerically are made after the proof of the theorem.

THEOREM 2.2. (a) *For $m \geq 2$, $0 < \beta < 1$, and γ a parameter, traveling waves can bifurcate from the synchronous solution at $\gamma = (1-\beta)/m$. For $m \geq 3$ and $\beta > 1$, traveling waves can bifurcate off the* S*-wave solution at $\gamma = (\beta - 1)/(m-2)$. See Fig.* 2 *for curves* 1 *and* 2. (*Due to the symmetry of the equation and ansatz with respect to the midpoint of the chain, both of these solutions arise from pitchfork bifurcations; i.e., waves can travel in either direction.*) *The bifurcations are supercritical; i.e., solutions exist for γ larger than the bifurcation value.*

(b) *For $\beta \ll 1$, there are $m-3$ curves of saddle nodes from which solutions to* (2.6) *bifurcate. When m is odd, these appear in pairs having the same image in the (β, γ) plane but corresponding to different values of $\bar{\phi}, \xi$. When m is even, the curves are distinct in the (β, γ) plane.* (*See Figs.* 3(a) *and* 3(b).)

(c) *For (β, γ) large but $\beta/\gamma = O(1)$, there are curves of saddle nodes. Along each of these curves, the end-to-middle phase lag ϕ_{em} is approximately an integer multiple of π. For m odd, there are $(m-3)/2$ distinct asymptotes, each corresponding to a pair of end-to-middle lags whose sum is approximately $m\pi$. Each such asymptote has a different slope. For m even, there are $m/2 - 1$ asymptotes with different slopes. They each correspond to a pair of end-to-middle phase lags that are approximately multiples of π and whose sum is approximately $m\pi$. The curve with end-to-middle phase lag about $m\pi/2$ is asymptotic to the γ axis.* (*See Figs.* 3(*a*) *and* 3(*b*).)

(d) *For $\gamma \to \infty$ or $m \to \infty$, there are solutions to* (2.6) *with $\bar{\phi}$ tending to a limit and $(\bar{\phi} - \xi) \to 0$. Any such solution has $\bar{\phi} \to k\pi/m$ for some integer k. If k is odd and $k < m/2$, the solution is stable.*

(e) *If γ and m are fixed, for β sufficiently large, the only solutions to* (2.6) *satisfying the hypotheses of Theorem* 2.1 *are the trivial ones ($\bar{\phi} = 0$; $\xi = 0, \pi$).* (*In particular, there are no traveling waves. See Fig.* 2.)

Proof. (a) Let β be fixed and γ be the bifurcation parameter. (A similar argument applies to γ fixed.) A necessary condition for bifurcation off a given solution is that the linearization of the left-hand side of (2.6) around that solution for some (β, γ) be noninvertible. For the synchronous solution, the matrix of the linearization is

$$M^+ = \begin{pmatrix} -1 + (m-1)\gamma & \gamma \\ -1 - (m-1)\beta & 1 - \beta \end{pmatrix}.$$

M^+ fails to be invertible when $\det M^+ = 0$. This occurs when $m\gamma + \beta = 1$. To show that the bifurcation actually occurs, we must consider higher-order terms. Let $\underline{e}$

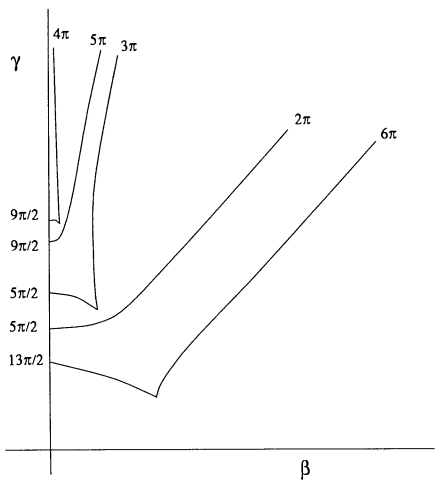

(a)

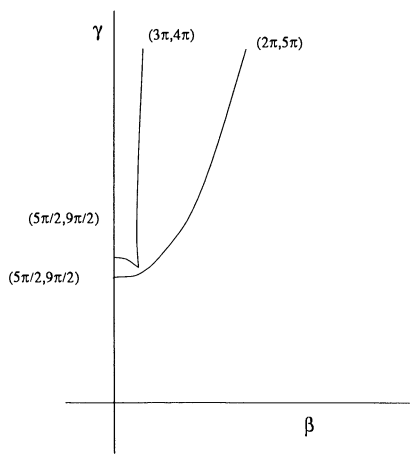

(b)

FIG. 3. *Schematic drawing of saddle-node curves, from analysis and numerics.* (a) $m = 8$. *Note that there are five points on the* γ *axis, as described in Theorem* 2.2(b). *The points are labeled by the end-to-middle phase lag* $\phi_{em} = (m-1)\overline{\phi} + \xi$. *Note that there are pairs of points with* ϕ_{em} *approximately* $9\pi/2$ *and* $5\pi/2$, *and a single solution with* $\phi_{em} \approx 13\pi/2$. *Within a pair, there is a difference in the relationship between* $\overline{\phi}$ *and* ξ. *For example, for* $\phi_{em} \approx 9\pi/2$, *the top solution has* $\overline{\phi} = \xi$ *and the lower one has* $\overline{\phi} = \pi - \xi$. *The five curves of saddle nodes for* $\beta \ll 1$ *are connected to five curves of saddle nodes for* β, γ *large, as described in Theorem* 2.2(c). *Each above pair with an end-to-middle phase lag of approximately* $(k + \frac{1}{2})\pi$ *comes near to a pair with end-to-middle lags of* $k\pi$ *and* $(k+1)\pi$, *with* $0 \le \xi \le \pi$. (*Numerical evidence suggests that the curves that come close do not actually touch one another, but they are closer than in the diagram, which was drawn for clarity. The numerics also indicate that all points on a given curve have lags between its* $\beta = 0$ *value and the associated asymptotic value.*) *The unpaired curve is connected to one with* $\phi_{em} \approx 6\pi$. *The curve with* $m\pi/2 \approx 4\pi$ *is asymptotic to the* γ *axis. For* β, γ *large, the curves exchange pairings with each new pair sharing a common asymptotic slope as* $\gamma, \beta \to \infty$, *and such that the sum of the* ϕ_{em} *is* 8π. *For general m even, the picture is similar, with the saddle-node curve having* $\phi_{em} \approx m\pi/2$ *asymptotic to the* γ *axis. An increase of m by two creates another pair of curves at* $\beta = 0$ *having a common* ϕ_{em} *at that point. The highest* ϕ_{em} *always corresponds to the lowest asymptotic slope.* (b) $m = 7$. *Each curve corresponds to two sets of saddle nodes. For the top pair on the* γ *axis,* $\overline{\phi} = \xi$; *for the bottom pair,* $\xi = \pi - \overline{\phi}$. *The values on the graph are again approximate values for* ϕ_{em}.

denote the eigenvector of the zero eigenvalue of M^+ at a parameter point (β,γ) satisfying $\gamma=(1-\beta)/m$, and let $\underline{l}$ be the left eigenvector. The quadratic terms of (2.6) vanish, so the leading-order nonlinear terms are cubic. Let $\underline{n}$ denote the cubic terms (which are homogeneous of order three) evaluated by setting each of the three inputs of a cubic term to $\underline{e}$. Let A be the linear term multiplying γ. Then a sufficient condition for supercritical bifurcation is that

$$\underline{l}\cdot A\underline{e}\neq 0, \qquad (\underline{l}\cdot\underline{n})/(\underline{l}\cdot A\underline{e})<0.$$

(This condition is valid when the quadratic terms are absent.) From the computation of M^+, we see that $\underline{e}=(1-\beta,1+(m-1)\beta)^T$ and $\underline{l}=(1-\beta,(\beta-1)/m)^T$. A is the 2×2 matrix with first row $(m-1,1)$ and second row zero. The cubic terms of (2.6) are

$$\frac{1}{6}\begin{pmatrix} \overline{\phi}^3-\gamma[(m-1)\overline{\phi}+\xi]^3 \\ \overline{\phi}^3-\xi^3+\beta[(m-1)\overline{\phi}+\xi]^3 \end{pmatrix},$$

from which $\underline{n}$ is derived by substituting the components of $\underline{e}$ for $\overline{\phi}$ and ξ. It is easily checked that $\underline{l}\cdot A\underline{e}=m(1-\beta)$, which is positive, provided that $0<\beta<1$. The numerator of the second condition for supercritical bifurcation is found (with the aid of MAPLE symbolic calculation software) to be

$$\underline{l}\cdot\underline{n}=-(1/6)(\beta-1)^2(m-1)[(m-2)\beta^2+(m+1)(\beta+1)],$$

which is strictly negative for $m\geq 2$.

For the S-wave solution, the corresponding matrix of the linearization is

$$M^-=\begin{pmatrix} -1-(m-1)\gamma & -\gamma \\ -1+(m-1)\beta & -1+\beta \end{pmatrix}.$$

M^- fails to be invertible when $\gamma(m-2)=\beta-1$. The left and right eigenvectors associated with M^- at a parameter point satisfying $\gamma=(\beta-1)/(m-2)$ are $\underline{e}=(-1+\beta,1-\beta(m-1))^T$ and $\underline{l}=(-1+\beta,(\beta-1)/(m-2))$. Calculations similar to those above show that, in this case, $\underline{l}\cdot A\underline{e}=(\beta-1)(m-2)>0$ and $\underline{l}\cdot\underline{n}=-(1/6)(m-1)(\beta-1)^2[m\beta^2+(m-3)\beta+(m-3)]$, which is negative for $m\geq 3$.

(b) We look for solutions to (2.6) other than the trivial solutions. To obtain explicit formulas, we first set $\beta=0$. From (2.6), we then have that $\overline{\phi}=\xi$ or $\overline{\phi}=\pi-\xi$. We perform our calculations separately for m odd and m even. First, assume that m is even. In the case where $\overline{\phi}=\xi$, the first equation of (2.6) states that

$$\sin\overline{\phi}=\gamma\sin(m\overline{\phi}). \tag{2.7}$$

This equation has precisely $m/2-1$ saddle nodes. The number of such saddle nodes is easily counted by looking for tangencies between the graphs of $\phi\to\sin\phi$ and $\phi\to\gamma\sin(m\phi)$ with $\gamma>0$; see Fig. 4(a). In the case where $\overline{\phi}=\pi-\xi$, the first equation is

$$\sin\overline{\phi}=-\gamma\sin[(m-2)\overline{\phi}]. \tag{2.8}$$

This equation has $(m-2)/2-1$ saddle nodes. (See Fig. 4(b).) Thus, for m even, the sum of the saddle-node solutions is $m-3$. For $\beta=0$, these points lie close to maxima of the curve $\phi\to\sin(m\phi)$ and $\phi\to-\sin[(m-2)\phi]$; this shows that the points are distinct.

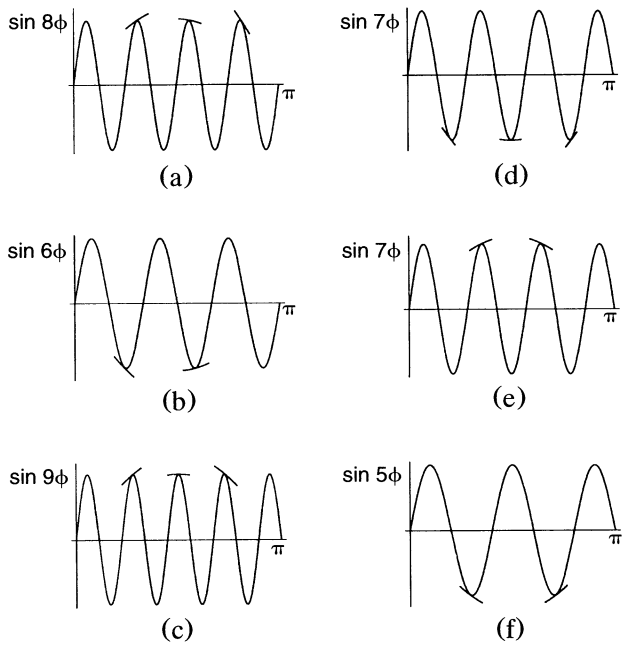

FIG. 4. *If* $\bar{\phi} = \xi$, *the saddle-node points occur for those values of* γ *for which there is a tangency between the graphs of* $\phi \to \sin\phi$ *and* $\phi \to \sin(m\phi)$. *These tangencies occur for values of* ϕ *near the maxima of* $\phi \to \sin(m\phi)$, *excluding the first maxima if* m *is even and the first and last if* m *is odd. See* (a), (c), *and* (e). *Similarly, for* $\phi = \pi - \xi$, (b), (d), *and* (f), *the saddle-node points occur for tangencies between* $\phi \to \sin\phi$ *and* $\phi \to -\gamma \sin[(m-2)\phi]$. *These tangencies occur near the minima of* $\phi \to \sin[(m-2)\phi]$ *excluding the last minima if* m *is even.* (a) $m = 8$, $\bar{\phi} \equiv \xi$. *Tangencies are near* $5\pi/16$, $9\pi/16$, $13\pi/16$. (b) $m = 8$, $\bar{\phi} \equiv \pi - \xi$. *Tangencies are near* $3\pi/12$, $7\pi/12$. (c) $m = 9$, $\bar{\phi} \equiv \xi$. *Tangencies are near* $5\pi/18$, $9\pi/18$, $13\pi/18$. (d) $m = 9$, $\bar{\phi} \equiv \pi - \xi$. *Tangencies are near* $3\pi/14$, $7\pi/14$, $11\pi/14$. (e) $m = 7$, $\bar{\phi} \equiv \xi$. *Tangencies are near* $5\pi/14$, $9\pi/14$. (f) $m = 7$, $\bar{\phi} \equiv \pi - \xi$. *Tangencies are near* $3\pi/10$, $7\pi/10$.

For m odd, the counting of saddle-node solutions to (2.7) and (2.8) depends on whether $m = 1 + 4k$ for some integer k or $m = 3 + 4k$ for an integer k. In the former case, there are $(k-1)$ values of γ for each of which there is a pair of saddle-node solutions satisfying $\bar{\phi} = \xi$; there is also an unpaired solution at $\gamma = 1$. If $\bar{\phi} = \pi - \xi$, there are again $(k-1)$ such values of γ plus an unpaired solution for $\gamma = 1$. (See Figs. 4(c) and 4(d).) The total number of solutions is $4(k-1) + 2 = 4k - 2 = m - 3$. In the case where $m = 3 + 4k$, there are k pairs of solutions for $\bar{\phi} = \xi$ and another k pairs for $\bar{\phi} = \pi - \xi$, for a total of $4k = m - 3$. (See Figs. 4(e) and 4(f).)

To show that the bifurcations are nondegenerate at $\beta = 0$, we indicate the results of the standard bifurcation calculation. Let M denote the linearization of (2.6) around one of the above saddle-node points, with $\bar{\phi} = \xi$. It can be checked that the right and left eigenvectors $\underline{e}$ and $\underline{l}$ are given by $(1,1)^T$ and $(m,-1)^T$. Since the bifurcations do not occur off $\bar{\phi} = 0$, the leading-order nonlinear terms in the Taylor expansion are now quadratic, shown below:

$$Q = \tfrac{1}{2}\begin{pmatrix} \sin(\bar{\phi})\tilde{\phi}^2 - \gamma_* \sin(m\bar{\phi})\left[(m-1)\tilde{\phi} + \tilde{\xi}\right]^2 \\ -\sin(\bar{\phi})\tilde{\phi}^2 + \sin(\bar{\phi})\tilde{\xi}^2 \end{pmatrix}.$$

Here γ_* denotes one of the bifurcation values of γ and $\tilde{\phi}, \tilde{\xi}$ are deviations from $\bar{\phi}, \xi$. Let A_1 and A_2 denote the vectors of partial derivatives of the left-hand side of (2.6) with respect to γ and β, respectively, evaluated at the point in question. The conditions for nondegeneracy are $\underline{l}\cdot A_1 \neq 0 \neq \underline{l}\cdot A_2$ and $\underline{l}\cdot Q(\underline{e},\underline{e}) \neq 0$. Since $\underline{l}\cdot A_1 = m\sin(m\bar{\phi})$ and $\underline{l}\cdot A_2 = \sin(m\bar{\phi})$, the first two conditions are satisfied. (At the saddle nodes, $\bar{\phi}$ satisfies $m\tan\bar{\phi} = \tan m\phi$. Thus $\sin(m\bar{\phi}) \neq 0$ for $0 < \tilde{\phi} < \pi$.) Also, using $\gamma_* \sin(m\bar{\phi}) = \sin\bar{\phi}$, we have $\underline{l}\cdot Q(\underline{e},\underline{e}) = [m(1-m^2)/2]\sin\bar{\phi} \neq 0$. These calculations show that the saddle-node curves extend beyond $\beta = 0$ and that the saddle nodes exist for points in the plane satisfying $\gamma > \gamma_*(\beta)$, where the latter denotes one of the $m-3$ curves of saddle nodes produced above. The argument is the same for $\bar{\phi} = \pi - \xi$. For m odd, the solutions that are paired at $\beta = 0$ continue to overlap in the β, γ plane. The reason is that, for m odd, (2.6) is invariant under $(\phi, \xi) \to (\pi - \phi, \pi - \xi)$; this gives rise to pairs of solutions along each bifurcation curve.

(c) Suppose now that $\beta, \gamma \gg 1$. Let $\gamma = \hat{\gamma}/\epsilon$ and $\beta = \hat{\beta}/\epsilon$. Dividing the first equation of (2.6) by γ and the second by β, we obtain

$$\begin{aligned} -(\epsilon/\hat{\gamma})\sin\bar{\phi} + \sin[(m-1)\bar{\phi} + \xi] = 0, \\ -(\epsilon/\hat{\beta})[-\sin\bar{\phi} + \sin\xi] - \sin[(m-1)\bar{\phi} + \xi] = 0. \end{aligned} \tag{2.9}$$

Using the first equation of (2.9), or (2.6), we can rewrite the second as

$$\left(1 + \frac{\beta}{\gamma}\right)\sin\bar{\phi} = \sin\xi. \tag{2.10}$$

For β, γ large, ϵ is $\ll 1$. At $\epsilon = 0$, the first equation of (2.9) implies that

$$(m-1)\bar{\phi} + \xi = \pi l \tag{2.11}$$

for some integer l. We may rewrite (2.10) and (2.11) as

$$\sin\bar{\phi} = \rho(-1)^{l+1}\sin[(m-1)\bar{\phi}], \tag{2.12}$$

where $\rho = \gamma/(\gamma+\beta)$. The number of double roots of (2.12), for all choices of $\rho \in (0,1]$ and both choices of sign, is computed as in part (b), above. Following clues from numerics, we seek solutions with $0 < \xi < \pi$; this, plus the value of $\bar{\phi}$, determines the end-to-middle lag and hence the value of l.

To understand the structure of the set of these bifurcation curves, we again distinguish between m odd and m even. Starting with the latter, the analysis in part (b) shows that there are $m-3$ tangent solutions, using both l odd and l even. (For $m = 8$, see Figs. 4(d) and (e) for the 5 tangent solutions.) These occur in pairs symmetric around $\pi/2$; this means that there are pairs of curves having the same asymptotic value for β/γ. There is an unpaired one at $\rho = 1$, $\phi = \pi/2$; note that $\rho = 1$ corresponds to $\beta = 0$, so that the asymptote for this curve, e.g., the one labeled 4π in Fig. 4(a) is the γ axis. Also, with $0 < \xi < \pi$, the end-to-middle phase lag $(m-1)\phi + \xi$ of that solution is $m\pi/2$, so $l = m/2$ for that solution. For the paired solutions, the values of $\bar{\phi}$ within a pair sum to π; with both values of ξ chosen near $\pi/2$, this implies that the values of the end-to-middle lags in a pair sum to approximately $m\pi$.

For m odd, we distinguish between $m = 4k+1$ for some k and $m = 4k+3$. Assume that $m = 4k+1$ and consider solutions with $\phi = \xi$. Then the saddle nodes, which are tangencies between the graphs of $\sin\phi$ and $\gamma\sin(m\phi)$, occur at $\phi = \pi/2$

for $\gamma = 1$ plus pairs of ϕ values symmetric around $\phi = \pi/2$ for some values of $\gamma < 1$. Saddle-node solutions with $\xi = \pi - \phi$ correspond to tangencies between the graphs of $-\sin\phi$ and $\gamma \sin[(m-2)\phi]$. Again, there is a single solution for $\gamma = 1$ and pairs for appropriate values of $\gamma < 1$. The total number is $m - 3$, and, for each value of γ (including $\gamma = 1$) for which there is a saddle-node bifurcation, there is a pair of values of ϕ. For $m = 4k + 3$, the analysis is similar, but $\gamma = 1$ is not a bifurcation value. A major difference between m odd and m even is that, for m odd, pairs of saddle-node curves overlap in the β, γ plane; for m even, the paired curves have only the same asymptotic value of β/γ. For m odd, the overlaps are forced by the symmetry considerations previously noted.

(d) First, let $\gamma \to \infty$, keeping m and β fixed. From (2.10), we have that $\bar{\phi} - \xi \to 0$ or $\bar{\phi} - (\pi - \xi) \to 0$. We will discuss only the former solutions, since the latter appear (numerically) to be unstable. Dividing the first equation of (2.6) by γ and letting $\gamma \to \infty$, we obtain $\sin(m\bar{\phi}) \to 0$ or, equivalently, $\bar{\phi} \to k\pi/m$ for some integer k. To show that there *are* such solutions, we must consider γ large, but finite. We now let $\epsilon = 1/\gamma$. The first equation of (2.6) is

$$-\epsilon \sin\bar{\phi} + \sin[(m-1)\bar{\phi} + \xi] = 0. \tag{2.13}$$

The limiting solutions as $\gamma \to \infty$ correspond to solutions for $\epsilon = 0$ to (2.13) and the second equation of (2.6). These can be considered as two equations in the three variables $\bar{\phi}$, ξ, and ϵ. It follows from a standard use of the implicit function theorem that solutions $\bar{\phi}(\epsilon), \xi(\epsilon)$ exist for small ϵ, with $\bar{\phi}(0) = 0$. The hypotheses of Theorem 2.1 are satisfied if k is odd and $< m/2$; the oddness of k is needed to ensure that $-\cos[(m-1)\bar{\phi} + \xi] > 0$, and $k < m/2$ keeps $\bar{\phi} < \pi/2$, so $\cos\bar{\phi} > 0$.

We now fix β and γ with $\gamma > 0$ and let $m \to \infty$. Recycling notation, we now let $\epsilon = 1/(m-1)$. Let $z \equiv (m-1)\bar{\phi}$. Equations (2.6) are then

$$\begin{aligned} -\sin(\epsilon z) + \gamma \sin(z + \xi) &= 0, \\ -\sin(\epsilon z) + \sin\xi - \beta \sin(z + \xi) &= 0. \end{aligned} \tag{2.14}$$

At $\epsilon = 0$, we have $\sin(z + \xi) = 0$, $\sin\xi = 0$. Thus as $m \to \infty$, $(m-1)\bar{\phi} + \xi \to k\pi$ for some integer k. To apply the implicit function theorem, we must calculate the linearization of (2.14) at $\epsilon = 0$; at this point, $z + \xi = k\pi$, so $\cos(z + \xi) = \pm 1$, depending on whether k is even or odd. Thus the matrix of the linearization is

$$\begin{pmatrix} \pm\gamma & \pm\gamma \\ -(\pm\beta) & \cos\xi - (\pm\beta) \end{pmatrix}.$$

The determinant of this matrix is nonzero, provided that $\cos\xi \neq 0$. Stability for k odd and $k < m/2$ again follows from Theorem 2.1.

(e) $\beta \to \infty$ implies that $(m-1)\bar{\phi} + \xi \to k\pi$ for some integer k. It also then follows from the first equation of (2.6) that $\sin\bar{\phi} \to 0$. Rescaling as above, we obtain a singular problem corresponding to $\beta = \infty$; since $\sin\bar{\phi} = 0$ for solutions to this singular problem, the only solutions satisfying the hypothesis of Theorem 2.1 (i.e., satisfying $|\bar{\phi}| < \pi/2$) are the trivial solution with $\bar{\phi} = 0$, $\xi = 0$ or π. For m finite, it follows from the implicit function theorem argument that there is a *unique* solution with β large near each such singular solution; since $\bar{\phi} = 0$ is such a solution, there are no others. □

Remark 2.1. The waves that bifurcate in Theorem 2.2(a) from a stable trivial branch appear numerically to inherit the stability; those bifurcating from an unstable branch inherit the instability. However, as the parameter γ increases, these waves stabilize. (See Fig. 2, curve 4 and Remark 2.7 following Theorem 2.3.) As mentioned previously, numerical evidence suggests that these traveling waves (the primary branch) tend for large γ or m to solutions with wavelength equal to the length of the chain.

Remark 2.2. Parts (b) and (c) of Theorem 2.2 describe the *origin* of families of traveling waves through saddle nodes. Part (d) describes stable families of traveling waves in parameter regimes different from those of parts (b) or (c). We do not fully understand how the different families are related as the parameters cross from one regime to another. We do, however, have partial information, particularly for $\beta \ll 1$, as in part (b). For $\beta = 0$, the solutions to (2.6) have $\xi = \bar{\phi}$ or $\xi = \pi - \bar{\phi}$, of which only the former are stable. The solutions satisfy (2.7). As γ increases, saddle nodes are formed. For $\gamma \gg 1$, each saddle node gives rise to a pair of solutions; the one with end-to-middle lag of $k\pi$, k odd, is stable. Numerical evidence suggests this account is also true for $\beta \neq 0$.

Remark 2.3. By symmetry, for every traveling wave with $\bar{\phi} > 0$, there is another wave (with $\bar{\phi} < 0$) traveling in the opposite direction.

Remark 2.4. We can numerically follow solutions to (2.6) as β increases. We find that the primary branch ($l = 1$) of the traveling wave solutions (stabilizing along curve 1 or curve 4, of Fig. 2, depending on the size of γ) meets a branch the bifurcates from the S-waves (at curve 2 or curve 7), with ξ going from 0 to π and $\phi \to 0$ as β increases. The secondary waves, which appear through saddle-node bifurcations, disappear through saddle nodes as β increases and γ is fixed.

Bifurcation, existence, and stability of antiwaves. Antiwave solutions, described by (2.5), have $m - 1$ variables. This makes the analysis considerably harder than for the traveling waves, in which the ansatz has only two variables, independent of m. As for the traveling waves, there are two types of results: the bifurcation results that describe the origin of the solutions as the variables β and γ cross bifurcation curves in parameter space, and asymptotic results for β, γ and/or m large. The bifurcation results here are weaker than those for antiwaves: We produce curves along which necessary conditions for bifurcation are satisfied, but we do not prove that the conditions are sufficient. Numerical calculations suggest that the necessary conditions are indeed sufficient. As in the traveling-wave case, the bifurcation results are more technical than the analysis for β, γ, or m large.

For large values of β or γ, we prove existence and stability of a family of antiwaves; in the limit, each of these has an end-to-middle phase lag of an integer multiple of π. The number of such families that we find increases linearly with m. The proof of these assertions (Theorem 2.3(c)) uses a continuum limit and scaled variables to show that there are solutions for finite (but large) β or γ. For m large, we use similar methods to analyze the behavior if solutions exist, but we do not provide constructions of solutions.

Substitution of (2.5) into (2.2) yields implicitly defined equations for the unknowns $\phi_1, \ldots, \phi_{m-1}$. These equations are

$$\begin{pmatrix} -2 & 1 & 0 & 0 & \cdots & 0 & 0 \\ 1 & -2 & 1 & 0 & \cdots & 0 & 0 \\ & \cdots & & & & & \\ 0 & 0 & 0 & 0 & \cdots & 1 & -2 \end{pmatrix} \begin{pmatrix} \sin \phi_1 \\ \sin \phi_2 \\ \vdots \\ \sin \phi_{m-1} \end{pmatrix} = \begin{pmatrix} -\gamma S \\ 0 \\ \vdots \\ -\beta S \end{pmatrix}, \tag{2.15}$$

where

$$S = \sin\left(\sum_{j=1}^{m-1} \phi_j\right) \equiv \sin \phi_{em}. \tag{2.16}$$

Note that S is the sine of the total phase lag ϕ_{em} from the end to the middle. The matrix in (2.15) is that of a discrete diffusion matrix with Dirichlet conditions. We can solve (2.15) to obtain the antiwave equation

$$\sin \phi_j = \frac{[\beta j + \gamma(m-j)]}{m} S. \tag{2.17}$$

THEOREM 2.3. (a) *For fixed $\beta > 0$, a necessary condition for bifurcation of antiwaves from synchrony is that $\gamma + \beta = 2/(m-1)$. (See Fig. 2, curve 5.) By symmetry, such a bifurcation must be a pitchfork, so, for any solution with waves traveling inward toward the center, there is a solution with the waves traveling outward.*

(b) *Along the line $\beta = \gamma$, a necessary condition for bifurcation is satisfied by a sequence of points at which the graph of $\phi \to \sin \phi$ is tangent to that of $\phi \to \gamma \sin [(m-1)\phi]$.*

(c) *As $\beta \to \infty$ or $\gamma \to \infty$, there are solutions for which the end-to-middle phase lag approaches a limit; for any of these, that limit is $k\pi$ for some k. These solutions exist and are stable for $\{(k, m)\}$ such that k is odd, m is sufficiently large, and $k < Cm$, for some constant $C < 1$ independent of m.*

(d) *Suppose that β and γ remain finite and $m \to \infty$. Then limiting values of solutions must have an end-middle phase lag of $k\pi$ for some integer k. The limiting form of such solutions satisfies an integral equation.*

Proof. (a) Linearize (2.16) and (2.17) around the synchronous solutions ($\phi_j \equiv 0$). For m fixed and solutions near enough, we have S also small. For x small, the linearization of (2.17) is

$$\phi_j = \frac{[\beta j + \gamma(m-j)]}{m} S.$$

Summing the series yields, for the linearized equations,

$$S = \left(\frac{\gamma + \beta}{2}\right)(m-1)S,$$

to which a nonzero solution S exists if and only if $\gamma + \beta = 2/(m-1)$.

(b) At $\beta = \gamma$, it follows from (2.17) that $\sin \phi_j = \gamma S$ for every j, so that $\phi_j \equiv \overline{\phi}$ for some $\overline{\phi}$. From (2.16), $S = \sin[(m-1)\overline{\phi}]$, and so from (2.17) we obtain $\sin \phi = \gamma \sin[(m-1)\phi]$. As in the proof of Theorem 2.2, a necessary condition for saddle-node bifurcation is satisfied at the sequence of points where the graph of $\phi \to \sin \phi$ is tangent to that of $\phi \to \gamma \sin[(m-1)\phi]$.

(c) We first show that, if a solution has a limiting end-to-middle phase lag, that limit must be $k\pi$ for some integer k and that the pair (m, k) must satisfy certain restrictions. We then show that, if those restrictions are met, there is indeed such a solution for β sufficiently large. For k even, the end-to-middle lag is far outside the region satisfying the hypotheses of the stability Theorem 2.1. Hence, we focus on k odd.

For β large and γ finite, let $\epsilon = 1/\beta$. Then (2.17) implies that

$$0 = \epsilon \sin \phi_j - \frac{[j + \gamma\epsilon(m-j)]}{m} S. \tag{2.18}$$

As $\epsilon \to 0$, we must have $S \to 0$, which implies the first assertion. To see that there are restrictions on the values of the integer k, we formulate the problem to use the implicit function theorem; the restrictions correspond to the zeroth-order stage of that calculation. We write

$$\hat{S} = \frac{1}{\epsilon} S = \frac{1}{\epsilon} \sin\bigl(k\pi + c_k \epsilon + O(\epsilon^2)\bigr). \tag{2.19}$$

Equations (2.18) are then

$$\sin \phi_j = \frac{[j + \gamma\epsilon(m-j)]}{m} \hat{S}. \tag{2.20}$$

At $\epsilon = 0$, (2.20) implies that $\{\phi_j\}$, $\hat{S}$ satisfy

$$\sin \phi_j = \frac{j}{m} \hat{S}, \tag{2.21a}$$

$$\sum_{j=1}^{m-1} \phi_j = k\pi. \tag{2.21b}$$

We now assume that k is odd. To see that (2.21) implies restrictions on (k, m), we note that (2.21), (2.19) must be solvable for c_k in the limit $\epsilon \to 0$. As a function of c_k, $\lim_{\epsilon \to 0} \hat{S}$ vanishes at $c_k = 0$ and is a monotone-decreasing function of c_k over some range of the latter. $|c_k|$ must be small enough that (2.21a) is solvable for all j. Indeed, since $\lim_{\epsilon \to 0} \hat{S} = -c_k$ and the largest value of the right-hand side of (2.21a) occurs for $j = m - 1$, we must have $[(m-1)/m]|c_k| < 1$. Thus, to solve (2.21b), the left-hand side of (2.21b) must be larger than $k\pi$ at the boundary of the interval of possible c_k. Since this boundary is $|c_k| = m/(m-1)$, this implies that m and k must satisfy the restriction

$$\sin^{-1}\left[\frac{1}{m-1}\right] + \sin^{-1}\left[\frac{2}{m-1}\right] + \cdots + \sin^{-1}(1) > k\pi. \tag{2.22}$$

Note that (2.22) fails for m small and $k > 1$. The left-hand side of (2.22), when divided by m, approaches the limit $\int_0^1 \sin^{-1}(x)\,dx$. Thus, the constant C providing the fraction is

$$\frac{1}{\pi} \int_0^1 \sin^{-1}(x)\,dx = \left(\frac{\pi}{2} - 1\right)\left(\frac{1}{\pi}\right).$$

We also note that the $\{\phi_j\}$ of these solutions lie in the primary branch of $\sin^{-1}(\cdot)$, i.e., $|\phi_j| < \pi/2$.

We now show that, if (2.21) is satisfied, then there are indeed antiwave solutions with end-to-middle lags approaching $k\pi$ and that these are stable. We consider (2.20) and the equation for $\hat{S}$ as m equations in the $m+1$ variables ϕ_j $(1 \le j \le m-1)$, c_k, and ϵ. We assume that (2.21) is satisfied, so we can solve those equations for $\{\phi_j\}$ and c_k at $\epsilon = 0$. We wish to solve (2.21a), (2.19) for $0 < \epsilon \ll 1$. Consider the matrix of the linearization of this system around the $\epsilon = 0$ solution. The last row of that matrix,

corresponding to the linearization of the equation for $\hat{S}$, has all zero entries, except for the last entry, which is $+1$ or -1, depending on whether k is even or odd. Omitting the last row and column, the resulting $(m-1)\times(m-1)$ matrix from (2.4a) is diagonal, with the jth entry $\cos\phi_j$. Since $\{\phi_j\}$ is constructed so that $|\phi_j| < \pi/2$ for every j, we have $\cos\phi_j > 0$. Hence the determinant of the matrix is nonzero, so the solutions exist. The solutions are stable by Theorem 2.1, providing that $-\cos(\Sigma\phi_j) > 0$, which is true if k is odd.

Now suppose that β stays finite but that $\gamma \to \infty$. The analysis is as before, with (2.21a) replaced by $\sin\phi_j = (1-j/m)\hat{S}$, whose largest value occurs now at $j=1$. The singular solutions are also the same as before, with the transformation $\phi_j \to \phi_{m-j}$. The implicit function theorem argument is as before.

(d) Now let γ and β be fixed, and $m \to \infty$. We show what the behavior of the solutions must be if there are solutions; however, the limiting argument does not construct the solutions. If there is to be any limit, we must have $\phi_j \to 0$ for each j. Hence, since (2.17) is true for all j, we must also have $S \to 0$, or $\phi_{em} \to k\pi$ for some integer k. To more fully understand the $\{\phi_j\}$, we let $\epsilon = 1/(m-1)$, $\phi_j = \epsilon\psi_j$. Then (2.17) becomes

$$\sin(\epsilon\psi_j) = \left[\gamma\left(1-\frac{j}{m}\right)+\frac{\beta j}{m}\right]S; \qquad S = \sin\left[k\pi + \epsilon L_k + O(\epsilon^2)\right]. \tag{2.23}$$

Dividing the first equation of (2.23) by ϵ and letting $\epsilon \to 0$, we obtain the singular equation

$$\psi(x) = (-1)^k[\gamma(1-x)+\beta x]L_k; \qquad \int_0^1 \psi(x)\,dx = k\pi. \tag{2.24}$$

Equations (2.24) may be solved for L_k and $\psi(x)$ for any positive integer value of k; for m finite, we expect solutions for some finite range of k, but this remains to be proved. □

Remark 2.5. The branch of antiwaves that bifurcates from the synchronous solution appears to exist as long as the local phase differences ϕ_j do not cross $\pi/2$, the turning point of $\sin x$. In simulations with short enough chains, the antiwaves do disappear with increasing β or γ. See §6.2.

Remark 2.6. Parts (a) and (b) of Theorem 2.3 give only necessary conditions for pitchfork and saddle-node bifurcations to antiwave solutions. These have been supplemented by numerical simulations. From these, we find that the antiwaves that bifurcate from synchrony exist for some range of $\gamma > -\beta + 2/(m-1)$. Similarly, in simulations there appear to be curves of saddle-node bifurcations through the points constructed in Theorem 2.3 (b), and the solutions born at such saddle-node curves exist for a range of values of γ larger than the values on those curves.

Remark 2.7. There is a critical value of γ and β at which both traveling waves and antiwaves bifurcate from synchrony, resulting in a double zero eigenvalue. Symmetry methods (see, e.g., [25]) can be used to unfold this degeneracy and resolve the stability of the two branches. We have not performed these calculations analytically, but include numerical results on the global bifurcation picture. (See Fig. 2, curves 3 and 4.) Other than in a neighborhood of this degeneracy, the antiwaves that bifurcate from a stable synchronous solution appear to be stable. If the synchronous branch is unstable (as a result of a traveling wave bifurcation), the antiwave branch is initially unstable, but it appears to stabilize as γ is increased.

Stabilization of S-waves. S-waves exist for all values of the parameters by symmetry, but they are stable only in some regions of parameter space. As shown in Proposition 2.1, S-waves are unstable for small enough long-distance coupling. Furthermore, by Theorem 2.2, traveling waves bifurcate from the S-waves as γ increases. The main result of this section is that, for $\gamma = 0$, the S-waves stabilize as β increases. Note that this does not follow from Theorem 2.1 because the first hypothesis of that theorem is not valid for the middle phase lag $j = m$. Nevertheless, we can prove the stability by making use of the structure of the equations to localize the eigenvalues enough to see that they have negative real part. We discuss the transition from unstable to stable and the effects of $\gamma \neq 0$ in remarks at the end of this section.

THEOREM 2.4. *Suppose that* $\gamma = 0$. *For* β *sufficiently large, the eigenvalues of the linearization of* (2.2) *around an* S*-wave are all in the left-hand plane. Of the* $2m-1$ *eigenvalues, two are* $O(\beta)$, *and the others are bounded as* $\beta \to \infty$.

Proof. The equations linearized around the S-wave solution have the following form:

$$(2.25)_1 \qquad -2x_1 + x_2 = \lambda x_1,$$

$$(2.25)_{m-1} \qquad x_{m-2} - 2x_{m-1} - x_m + \beta \sum_{j=m}^{2m-1} x_j = \lambda x_{m-1},$$

$$(2.25)_m \qquad x_{m-1} + 2x_m + x_{m+1} - \beta \sum_{j=1}^{m} x_j - \beta \sum_{j=m}^{2m-1} x_j = \lambda x_m,$$

$$(2.25)_{m+1} \qquad -x_m + 2x_{m+1} + x_{m+2} + \beta \sum_{j=1}^{m} x_j = \lambda x_{m+1},$$

$$(2.25)_{2m-1} \qquad x_{2m-2} - 2x_{2m-1} = \lambda x_{2m-1},$$

$$(2.25)_j \qquad x_{j-1} - 2x_j + x_{j+1} = \lambda x_j,$$

where the last equation holds for $j \neq 1,\ m-1,\ m+1,\ 2m-1$. We let $\epsilon = 1/\beta$ and $\bar{\lambda} = \epsilon\lambda$. Multiplying (2.25) by ϵ and letting ϵ tend to zero, we are left with a matrix $\bar{M}$ of coefficients, whose rows are entirely zero except for those corresponding to $j = m-1,\ m,\ m+1$. These rows are

$$(0,\ldots,0,1,1,\ldots,1),$$
$$(-1,\ldots,-1,-2,-1,\ldots,-1),$$
$$(1,\ldots,1,1,0,\ldots,0).$$

The eigenvalues $\bar{\lambda}$ are zero (with multiplicity $2m-3$) and -1 (with multiplicity 2); the latter statement can be checked by noting that the associated eigenvectors are $(0,0,\ldots,0,1,0,-1,0,\ldots,0)$ and $(0,\ldots,0,1,-2,1,0,\ldots,0)$. For β large, the eigenvalues -1 perturb to other eigenvalues in the left half-plane. To show stability, we must show that the remaining $2m-3$ eigenvalues perturb to values in the left-hand plane.

We return now to the original equations (2.25). We are interested in the eigenvalues that remain regular as $\beta \to \infty$ and we start by computing their limiting values. Using the ansatz $x_j = \sin \alpha j$ for the components of an eigenvector, where α is to be determined, $(2.25)_j$ implies that λ is then $2[\cos\alpha - 1]$. This ansatx is motivated by the fact that, in the absence of the β terms, up through the $m-1$th row, the linearized matrix is equal to that of the discrete diffusion matrix with zero Dirichlet

conditions; the latter matrix has eigenvectors of that form and of the above eigenvalues. We show that, for large β, the limiting eigenvalues and eigenvectors of (2.25) do satisfy this ansatz.

Let M be the matrix of coefficients in (2.25). M is symmetric around $j = m$, so we can calculate the eigenvalues by splitting the space into sums of eigenvectors that are either symmetric ($x_j = x_{2m-j}$) or antisymmetric ($x_j = -x_{2m-j}$). First, note that, for each eigenvalue $\bar{\lambda}$ that goes to zero with ϵ, the corresponding λ is bounded. Consider now an eigenvector associated with such a λ, with components $\{x_j\}$ that are themselves bounded. From $(2.25)_{m-1}$ and $(2.25)_{m+1}$, we then have that $\sum_{j=1}^{m} x_j$ and $\sum_{j=m}^{2m-1} x_j$ are $O(1/\beta)$.

We start with the antisymmetric subspace, which has dimension $m-1$. Antisymmetry implies that $x_m = 0$ and $x_{m+1} = -x_{m-1}$. Therefore the first $m-1$ equations of (2.25) decouple from the rest. However, $(2.25)_{m-1}$ does not constrain the solutions to lowest order, because high-order changes to $\{x_j\}$ can change the $O(1)$ value of $\beta \sum_{j=m}^{2m-1} x_j$. Indeed, for the limiting solution for regular eigenvalues, we can replace that equation by

$$\sum_{j=1}^{m} x_j = 0. \tag{2.26}$$

The first $m-2$ equations of (2.25) are satisfied by the ansatz (for the eigenvalues and eigenvectors) for any value of α. Using $x_m = 0$ and the ansatz $x_j = \sin(\alpha j)$, (2.26) is equivalent to

$$\sum_{j=1}^{m-1} \sin(\alpha j) = 0,$$

which, in turn, is equivalent to

$$\sin(m\alpha) - \sin[(m-1)\alpha] - \sin\alpha = 0. \tag{2.27}$$

The solutions to (2.27) are $\alpha = 2\pi k/m$, $k = 1, \ldots, m/2$ and $\alpha = 2\pi k/(m-1)$, $k = 1, \ldots, (m-1)/2$, where we do not include π among the possible roots. There are $m-2$ such roots. For the above values of α, the associated values of λ have negative real part. Since the roots are all simple, they and the associated eigenvalues perturb for small $1/\beta$ by $O(1/\beta)$.

We now consider the subspace of symmetric solutions. The first m equations of (2.25) then decouple from the rest. This time both $(2.25)_{m-1}$ and $(2.25)_m$ are each unconstraining of the lowest-order part of the solution. In the limit, we have (2.26) as before, which we can write as

$$x_m = -\sum_{j=1}^{m-1} x_j. \tag{2.28}$$

We also have one more equation that comes from combining $(2.25)_{m-1}$ and $(2.25)_m$ to eliminate the common terms that are dependent on higher-order perturbations. Inserting the ansatz, we find that the first $m-2$ equations are again satisfied by the ansatz for any value of α. Using x_m as in (2.28), the combined equation becomes

$$(1+\lambda)\sin[\alpha(m-1)] - \sin[\alpha(m-2)] = \frac{\lambda}{2} \sum_{j=1}^{m-1} \sin(\alpha j).$$

Using trigonometric identities as above, the latter can be shown to be equivalent to

$$\sin(m\alpha) - \sin[(m-1)\alpha] + \sin\alpha = 0. \tag{2.29}$$

The roots of (2.29) are $\alpha = (2k-1)\pi/m$, $k = 1,\ldots,m/2$ and $\alpha = (2k+1)\pi/(m-1)$, $k = 1,\ldots,(m-1)/2$. There are $m-1$ such roots, and the associated eigenvalues lie in the left-hand plane. Again, for large values of β, the roots perturb by $O(1/\beta)$, and hence the associated eigenvalues remain in the left-hand plane. □

Remark 2.8. For $\gamma = 0$, the stabilization of S-waves as β increases is somewhat complicated, and depends on the length of the chain. In numerical experiments, we have found that, for short chains ($m = 1,2,3$), the S-wave becomes stable as β passes through $\beta = 1$, where there is a degeneracy in (2.2). For longer chains and $\beta < 1$, there is a single positive eigenvalue. At $\beta = 1$, a zero eigenvalue appears (with the mth unit vector as its eigenvector). As β increases further, the zero eigenvalue moves back into the right-hand plane; however, still further, two real positive eigenvalues coalesce, then become complex, and move so as to cross the imaginary axis at some $\beta = \beta_H$, producing an inverse Hopf bifurcation that stabilizes the S-waves. For all $\beta > \beta_H$, the S-wave is stable.

Remark 2.9. We have also numerically considered the behavior for $\gamma \geq 0$. For $\beta\epsilon(\beta_\infty(\gamma), \beta_H(\gamma))$, there are periodic solutions to (2.2), which we call "S-wobbles," that bifurcate supercritically from S-waves as γ is increased from $\gamma = 0$. As β decreases for $\gamma \geq 0$ fixed, such a periodic solution appears to die at some $\beta_\infty(\gamma)$ on an infinite period solution. As β increases, it dies by an inverse Hopf bifurcation at $\beta_H(\gamma)$. $\beta_\infty(0) = 1$ and $\beta_H(0) = 2$, so there is a region of S-wobbles even for $\gamma = 0$. At least for $m = 8$, the points $\beta_\infty(\gamma)$ and $\beta_H(\gamma)$ come together at some finite value of γ, beyond which there are no more S-wobbles. An S-wave that is stable at $\gamma = 0$, β large loses stability to a traveling wave as γ is increased (see Theorem 2.2); this happens through a zero eigenvalue. See Fig. 2, curves 6 and 7.

Half chains. In [5] Cohen, Holmes, and Rand also discussed chains with local coupling and sparse long-range coupling, using the same functions as in this paper for short- and long-range coupling. In that paper, the long-range connections are between the end two oscillators, and the coupling from the first to the last has the same strength as that from the last to the first. We show here the sense in which the work of this section constitutes a generalization to that work. In particular, we show that with the connectivity as in [5], even if the two long-range connections have *different* strengths, the analysis reduces to that of traveling wave and antiwave solutions given above.

By a "half-chain," we mean a chain of length N with inhibitory connections between the two ends (as opposed to connections between the ends and the middle). For such connectivity, we let β be the strength of the connection from oscillator 1 to N and γ the strength from N to 1. Let $N \equiv m-1$. Then the equations are exactly (2.15). Thus each antiwave solution for the full chain provides a solution for the half-chain. Recall that these solutions have ϕ_j varying with j, so they do not give rise to constant-speed traveling waves. There are additional solutions if $\beta \approx \gamma$. For $\beta = \gamma$ [5], the traveling wave ansatz $\phi_j \equiv \bar{\phi}$ leads to (2.6) with $\xi = 0$.

3. Long chains and unsymmetric perturbations. All the results of §2 were obtained under hypotheses of strict symmetry on the equations. Since the solutions obtained are asymptotically stable, the qualitative behavior must remain under perturbations that remove some features of the symmetry. However, for long chains,

the solutions may change under perturbation. The central result of this section is that the qualitative behavior of the antiwaves does not persist for long chains if the local coupling is anisotropic, i.e., if the coupling from the kth oscillator to the $(k-1)$th is not the same as the coupling from the kth to the $(k+1)$th. More explicitly, we derive the natural equations for a continuum limit of such solutions and show that, if the local coupling is anisotropic, there cannot be antiwave solutions. The arguments do not rule out traveling waves, but place some restrictions on them. For this work, the local and global coupling functions are allowed to be more general than the specific functions used in the previous section.

A continuum limit for antiwave solutions. A continuum limit description is appropriate for solutions such as antiwaves in which the middle-to-end phase lag approaches a limit as $m \to \infty$ and whose phase lags ϕ_j vary in a manner consistent with the discretization of a continuous function. We are looking for a continuous function $\Theta(x)$ defined for $0 \le x \le 1$ such that $\Theta(j/2m) \approx \theta_j$. If there is to be a limiting value for the end-to-middle lag, the lags must each be small, except perhaps for those near the ends or middle of the chain. Thus, the natural continuum limit of $(2.1)_j$, $j \neq 1, m, m+1, 2m$ is

$$\text{(3.1)} \qquad \overline{\Omega} = \Delta(\alpha^+ - \alpha^-)\Theta_x + \frac{\Delta^2}{2}\left[(\kappa^+ - \kappa^-)\Theta_x^2 + (\alpha^+ + \alpha^-)\Theta_{xx}\right] + o(\Delta^2),$$

where $\Delta = 1/2m$, $\alpha^{\pm} = (h^{\pm})'(0)$, $\kappa^{\pm} = (h^{\pm})''(0)$, and $\overline{\Omega}$ is the phase-locked frequency. (Equation (3.1) is derived from $(2.1)_j$ by writing $\theta_{j\pm1} = \theta_j \pm \Delta\theta_x + (\Delta^2/2)\theta_{xx} + o(\Delta^2)$ and using a Taylor expansion through $O(\Delta^2)$.) Note that, if the medium is isotropic, then $\alpha^+ = \alpha^-$, so the terms of order Δ cancel. We also note that the assumptions on $h^{\pm}$ in the stability Theorem 2.1 guarantee that the coefficient of Θ_{xx} is positive. Such a continuum description is consistent with the equations for $j = 1, m, m+1, 2m$, provided that $|\theta_{m+1} - \theta_1| \to \pi$, $|\theta_m - \theta_{2m}| \to \pi$, and $f^{\pm}(\pi) = 0 = g^{\pm}(\pi)$, as in the coupling we have been using.

Suppose that the medium is anisotropic, so that the coefficient of Θ_x is nonzero. Then the first term on the right-hand side of (3.1) dominates the others. Rescaling $\overline{\Omega}$ by defining $\overline{\Omega} = \Delta\Omega$, we have the equation expected to be valid away from boundary layers,

$$\text{(3.2)} \qquad \Omega = (\alpha^+ - \alpha^-)\Theta_x.$$

It is immediate from (3.2) that such a description is incompatible with antiwaves. The reason is that Ω, the scaled phase-locked frequency, is independent of x and must be the same on both sides of the antiwave. However, (3.2) then implies that the phase gradient has the same sign on both sides of the middle of the chain, which contradicts the defining property of antiwaves. We can summarize this discussion in the following proposition.

PROPOSITION 3.1. *Suppose that the local coupling in* (2.1) *is anisotropic and that the long-range coupling functions vanish at* 0 *and* π. *Then the continuum limit equations* (3.1) *have no solutions representing antiwaves.*

Remark 3.1. Numerical simulations suggest that traveling waves continue to exist for the anisotropic regime. Away from the ends and the middle, they appear to satisfy (3.2) with the end-to-middle lag approximately $k\pi$ for some k odd.

Remark 3.2. The continuum limit used in this section differs in an important way from that of [7] and [15]. When there is only local coupling, as in the latter papers, the

total phase lag does not approach a limit as the strength of the chain grows without bound; instead, it is the individual lags that approach such a limit. The appropriate continuum limit for the latter situation keeps the coupling strength between successive oscillators constant as the size grows, unlike the current situation in which the strength scales like discretization of derivatives.

Finite chain perturbations. For any given chain size, the stable solutions (and the hyperbolic ones as well) perturb with changes of the equation. However, the size of the allowable perturbation of the equation can a priori go to zero as the chain grows in size. To explore this, we did numerical simulations with variations on the equations investigated analytically. We found that, if we keep the coupling "diffusive" (i.e., $h^{\pm}(0) = 0$, although $h^{\pm}$ need not be odd functions), then the S-waves and the traveling waves persist even for long chains. (The bifurcation diagrams change, of course, e.g., the pitchfork bifurcation of the traveling waves is no longer symmetric.) By contrast, the antiwaves are much less robust. In particular, in simulations using $h^{+} \neq h^{-}$, the antiwaves disappear for long enough chains. This is consistent with the continuum limit analysis presented earlier in this section. We have not been able to understand the behavior of perturbed systems in which the coupling is not diffusive.

4. Chains with one-point inhibition. We now consider a different connection topology, in which the long connections from and to both ends go to a single oscillator, rather than to a pair. We find some major differences in the behavior of the chain.

To take advantage of the simplicity afforded by symmetries, it is now useful to work with an odd number of oscillators, and we let $N = 2m + 1$. The equations are now

$$(4.1)_j \qquad \frac{d\theta_j}{dt} = \omega + h^{+}(\theta_{j+1} - \theta_j) + h^{-}(\theta_{j-1} - \theta_j)$$

for $j \neq 1,\ m+1,\ 2m+1$. The remaining equations are

$$(4.1)_1 \qquad \frac{d\theta_1}{dt} = \omega + h^{+}(\theta_2 - \theta_1) + f^{+}(\theta_{m+1} - \theta_1),$$

$$(4.1)_N \qquad \frac{d\theta_N}{dt} = \omega + h^{-}(\theta_{N-1} - \theta_N) + f^{-}(\theta_{m+1} - \theta_N),$$

$$(4.1)_{m+1} \qquad \frac{d\theta_{m+1}}{dt} = \omega + h^{+}(\theta_{m+2} - \theta_{m+1}) + h^{-}(\theta_m - \theta_{m+1}) + g^{-}(\theta_1 - \theta_{m+1}) + g^{+}(\theta_N - \theta_{m+1}).$$

The functions $h^{\pm}$, $f^{\pm}$, and $g^{\pm}$ are as in §2.

Before we perform the analysis, we must first give the appropriate meaning of traveling waves and antiwaves. We note that there is no analog of S-waves for this connection topology; without an overlap, there is no possibility of domains of synchrony separated by antiphase in phase-difference coupled equations. (Such domains are possible even with nearest-neighbor architecture for relaxation oscillators coupled with some classes of coupling [26]; they are also possible for limit cycle oscillators with long-range inhibition, provided that there is an amplitude variable that can go to zero at the interface of the domain [27].) Nor have we found any new family of solutions that exists for this connectivity, but not the overlap connectivity of §2. See Fig. 5 for the bifurcation diagram.

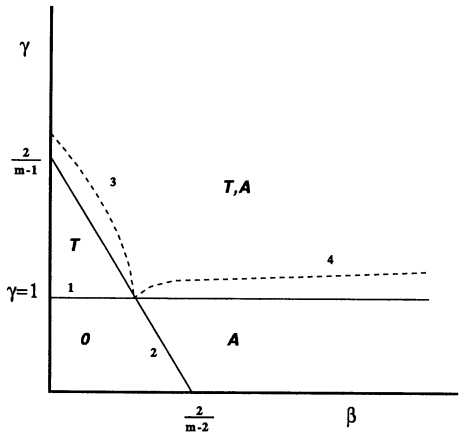

FIG. 5. *Schematic bifurcation diagram for one-point inhibition. Symbols mean: T, traveling waves; A, antiwaves; 0, synchrony.* (1) *Pitchfork bifurcation to stable traveling waves from synchrony.* (2) *Pitchfork bifurcation to antiwaves from synchrony.* (3) *Stabilization of antiwaves via secondary bifurcation (numerical).* (4) *Stabilization of traveling waves through secondary bifurcation.*

By a traveling wave, we mean a solution of the form

$$\phi_j = \bar{\phi} \neq 0, \pi \quad \text{for } j \neq m, m+1; \qquad \phi_m = \phi_{m+1} = \xi. \tag{4.2}$$

Antiwaves are solutions of the form

$$\phi_j = -\phi_{2m-j+1}. \tag{4.3}$$

We treat solutions of the form (4.2) and (4.3) together in the next theorem. The methods are similar to those of Theorem 2.2, but the analysis is much easier.

THEOREM 4.1. (a) *For small enough γ and β, the only stable phase-locked solutions are synchronous.*

(b) *Traveling waves correspond to nontrivial solutions to*

$$\sin \bar{\phi} = \gamma \sin(m\bar{\phi}). \tag{4.4}$$

A branch of such traveling waves bifurcates from synchrony at the line $\gamma = 1/m$, and other branches arise from saddle-node bifurcations at higher values of γ. Such a solution is stable if $0 < \bar{\phi} < \pi/2$ and $\bar{\phi}$ lies on a branch of $\sin(m\phi)$ having negative slope. For γ sufficiently large, there are approximately $m/4$ such stable solutions, and, as $\gamma \to \infty$, the stable solutions have an end-to-middle phase difference that approaches $k\pi$, where k is an odd integer.

(c) *Antiwaves satisfy the implicitly defined equations* (2.20), *where S is now*

$$S = \sin\left(\sum_1^m \phi_j\right). \tag{4.5}$$

A necessary condition for bifurcation from synchrony is satisfied if

$$\gamma m + \beta(m+1) = 2 + \frac{1}{m}. \tag{4.6}$$

At $\beta = \gamma$, a necessary condition for bifurcation is satisfied for values of γ and ϕ such that the graph of $\phi \to \sin\phi$ is tangent to that of $\phi \to \gamma \sin(m\phi)$. For γ large, there are antiwave solutions, and their end-to-middle phase lag approaches a multiple of π; such a solution is stable if that multiple is odd.

Proof. (a) Corollary to Proposition 2.1.

(b) Solutions satisfying (4.1), (4.2) must satisfy the analog of (2.6), namely,

$$\begin{aligned} -\sin\bar{\phi} + \gamma \sin[(m-1)\bar{\phi} + \xi] &= 0, \\ -\sin\bar{\phi} + \sin\xi &= 0. \end{aligned} \tag{4.7}$$

The second equation of (4.7) implies that $\phi = \xi$ or $\phi = \pi - \xi$, and we discuss only the former, since the latter appears (numerically) to be unstable. Equation (4.4) is now immediate. The assertions about the bifurcations follow from considerations of the graphs of $\sin\phi$ and $\gamma\sin(m\phi)$, as in §2. The asymptotic stability follows from Theorem 2.1, since the slope of the graph of $\sin(m\phi)$ specifies the sign of the relevant derivatives in the hypotheses. That there are approximately $m/4$ such stable solutions for γ sufficiently large follows from the fact that the graph of $\gamma\sin(m\phi)$ has approximately $m/4$ positive sections in the interval $0 < \phi < \pi/2$, and for γ large enough each such section intersects the graph of $\sin(\phi)$ exactly once at a point of negative slope of $\gamma\sin(m\phi)$. As $\gamma \to \infty$, the intersections approach $k\pi/m$, for k an odd integer, so the end-to-middle phase lag approaches $k\pi$.

(c) Substituting (4.3) into (4.1) yields equations for $\{\phi_j\}$. These equations are similar to (2.15), this time for an $m \times m$ system whose first $m-1$ equations are those of (2.15), and mth is $\sin\phi_{m-1} - 3\sin\phi_m = -2\beta S$. The solution to these equations is

$$\sin\phi_j = \frac{2\beta j + \gamma(2m+1-2j)}{2m+1} S.$$

To compute the bifurcation from synchrony, we linearize these equations around $\phi \equiv 0$. Summing the series for S, we then have the linearized condition

$$\frac{m}{2m+1}[m\gamma + \beta(m+1)]S = S.$$

This has a nonzero solution if and only if (4.6) is satisfied.

If $\beta = \gamma$, then $\phi_j \equiv \bar{\phi}$, independent of j, as in §2. Then $S = \sin(m\bar{\phi})$, so saddle-node bifurcations can occur only where (4.4) and its derivative with respect to $\bar{\phi}$ are both zero, i.e., where there are tangencies of the graphs of $\sin\phi$ and $\gamma\sin(m\phi)$. For γ large, the proof of existence of antiwave solutions is as in §2, as is the proof of asymptotic stability. □

Remark 4.1. The bifurcation analysis for the traveling waves is much simpler in the one-point inhibition case because (4.7) does not have the terms of (2.6) involving β. The bifurcation curves are thus independent of β, and there is not the complex interplay of bifurcation curves displayed in Figs. 4(a) and 4(b). In this case, it is much clearer where the stable solutions originate, and we may ignore a priori the solutions originating with $\xi \approx \pi$.

Remark 4.2. The continuum limit analysis is as in §2.

5. Translation-invariant coupling. We now turn to another topology for the long-range coupling. For this topology, the coupling between θ_1 and a middle oscillator θ_{m+1} is repeated between θ_j and θ_{m+j}, for each j such that $m+j \le N$. Similarly, coupling between the end oscillator and a middle oscillator is also repeated

in a translation-invariant way. As in the previous parts of this paper, such coupling can be done in two ways, with a pair of central oscillators as in §2, or a single central oscillator as in §4. In this section, we present numerical studies concerning the behavior of chains with such architectures. We find traveling wave and antiwave solutions very similar to those that occur with the more sparse coupling of §§2 and 4. However, in this case, antiwaves appear to be far less robust and were found only in small parameter regimes. The work reported in this section is entirely numerical.

The local coupling is given as before by $h(\phi) = h^+ = h^- \equiv \sin\phi$. Instead of inward and outward coupling, we now have descending and ascending coupling $F(\phi) = -\sin\phi = G(\phi)$, with coupling strengths δ and α. The phase differences ϕ_j are defined as before. For coupling with a pair of middle oscillators, and $N = 2m$, the equations for the $\{\phi_j\}$ take the form

$$\frac{d\phi_j}{dt} = h(\phi_{j+1}) - h(\phi_j) + h(-\phi_j) - h(-\phi_{j-1}) + \alpha\left[F\left(\sum_{k=1}^{m}\phi_{k+j}\right) - F\left(\sum_{k=0}^{m-1}\phi_{k+j}\right)\right]$$

for $j = 2,\ldots,m-1$,

$$\frac{d\phi_j}{dt} = h(\phi_{j+1}) - h(\phi_j) + h(-\phi_j) - h(-\phi_{j-1}) + \delta\left[G\left(-\sum_{k=1}^{m}\phi_{k+j}\right) - G\left(-\sum_{k=0}^{m-1}\phi_{k+j}\right)\right]$$

for $j = m+1,\ldots,2m-2$. The remaining equations are

$$\frac{d\phi_1}{dt} = h(\phi_2) - h(\phi_1) + h(-\phi_1) + \alpha\left[F\left(\sum_{k=1}^{m}\phi_{k+1}\right) - F\left(\sum_{k=0}^{m-1}\phi_{k+1}\right)\right],$$

$$\frac{d\phi_m}{dt} = h(\phi_{m+1}) - h(\phi_m) + h(-\phi_m) - h(-\phi_{m-1}) + \delta G\left(-\sum_{k=1}^{m}\phi_k\right) - \alpha F\left(\sum_{k=0}^{m-1}\phi_{k+m}\right),$$

$$\frac{d\phi_{2m-1}}{dt} = -h(\phi_{2m-1}) + h(-\phi_{2m-1}) - h(-\phi_{2m-2}) + \delta\left[G\left(-\sum_{k=1}^{m}\phi_{k+j}\right) - G\left(-\sum_{k=0}^{m-1}\phi_{k+j}\right)\right].$$

We start by discussing the isotropic case where $\alpha = \delta$. As in the other topologies, the synchronized solution is stable only for α small, with bifurcations occurring at a value that tends to zero as the chain size grows without bound. Traveling waves bifurcate stably at some value $\alpha = \alpha_T$ and remain stable for all values of $\alpha > \alpha_T$. Near the bifurcation value, the unstable eigenfunction has the approximate form $\phi_j \approx \sin(\pi j/2m)$. As α increases, the $\{\phi_j\}$ remain positive and tend to a constant $\bar{\phi} \approx 2\pi/(2m-1)$, the uniform traveling wave.

If we continue to follow the synchronous branch beyond the first bifurcation, we find a second bifurcation with an eigenvector that is approximately $\phi_j \approx \sin(2\pi j/2m)$. This solution is antisymmetric around the center of the chain and hence represents an antiwave. Since the bifurcation occurs from an unstable solution, it is itself unstable; however, after further increases in α, the solution stabilizes (at a value α_A). Still further increases in α cause the antiwaves to coalesce with an unstable branch of solutions; thus the antiwaves persist for only a small range of values of α. For example, if $N = 12$, the antiwaves exist for $\alpha \in (0.36, 0.58)$.

We now consider the effect of anisotropy, i.e., $\alpha \neq \delta$. For α fixed and δ decreasing, the traveling wave persists, but it loses its symmetry around the center. The wave exists for all δ down to $\delta = 0$ and remains stable. If δ is decreased from $\delta = \alpha$ in the range where stable antiwaves exist for the isotropic case, the stable antiwaves continue for some interval of δ and then merge with an unstable branch in a saddle-node bifurcation and disappear. The size of the ratio δ/α appears to make little difference in the robustness of the stable antiwaves.

We have been unable to obtain stable S-waves for this topology and conjecture that they cannot exist, though unstable S-waves do exist. We also did not find any dynamic phenomena, such as S-wobbles. We found no major differences between the two-center and one-center topologies when there is translational invariant coupling.

6. Discussion.

6.1. Chains of oscillators and neural development in vertebrates. In §1 we discussed observations on motor behavior during early development. We now use some of the mathematics from the previous sections to produce a speculative account of how such a sequence of changes could take place. It must be cautioned that the mathematics describes neural behavior, while the observations were made about mechanical behavior; it is known that the transformation between the neural activity and the mechanical activity that it causes is not necessarily straightforward [28]. With that caveat, we identify the observations on mechanics with the behavior of the neural network.

The rhythmic C-coils that appear very early correspond to synchronous oscillatory contractions of the muscles all along the spinal cord. It was shown in [7] that a chain of oscillators coupled locally using coupling modeled on diffusion produces such synchrony. Furthermore, electrical junctions that provide this kind of coupling are believed to be very common in early development [29], [30]. Finally, the local coupling (sine of phase differences) that we use in our models is the outcome of the reduction process that produces (2.1) when the physical coupling is diffusion and the oscillators have some symmetry properties [16]. Thus the local coupling that we use is a reasonable phenomenological description of coupling action during very early development and produces the observed C-coil behavior.

This paper shows that the traveling waves and S-waves associated with the later stages of development could occur as a consequence of fairly simple changes in architecture involving the addition of some long fibers whose connections are designed to create antiphase behavior between the two oscillators directly coupled. Those long fibers need not go precisely to and from the middle; any position roughly near the middle with long fibers overlapping will do. For example, suppose that the long fibers grow from the ends, and synapses made en passant do not become functional (or permanent) until the two sets of inwardly growing fibers reach a common area. These inward fibers could give rise to the S-waves and intermediate stages described above. If fibers following the paths of the inward fibers then grow

outward from the middle, traveling waves also become possible. Though there are many such waves possible, the wave with wavelength equal to body length occurs first.

The long fibers discussed above cannot be the only mechanism giving rise to the production of traveling waves of locomotion, at least for adult lampreys. The reason is that parts of the spinal cord that are considerably shorter than half the total length are still capable of self-organizing into a traveling wave with an unchanged phase lag between two given points [4]. We note that the traveling waves produced during development might act as a "teaching signal," which could then be used by the animal at a later stage to create local connections that could produce the waves without the long fibers. Models showing that such "learning" of phase lags is possible are in [31].

There are other wave-like phenomena exhibited by other species that display undulatory swimming. A number of electric fish retain the ability to produce waves more complicated than traveling waves on a dorsal or ventral fin [32]. Like antiwaves, these waves can have as leading oscillator one in the middle of a fin, with waves progressing outward; unlike our waves, the leading oscillator can itself change position. For more phenomenological descriptions of oscillators in development, see [33]. We also note that the "intermediate" behavior in development that we described in the Introduction has not been well characterized, leading to terminology that is not well specified: e.g., S-wave is used in the biological literature to denote a range of behaviors, including what we have here called S-waves and antiwaves [23].

6.2. Chain size and scaling. We have seen that "short" chains can exhibit some emergent behaviors that are not found in longer ones. (See Remarks 2.5 and 2.8). For example, we have seen that, in the overlap topology with nearest-neighbor coupling, antiwaves exist in some short chains ($m \leq 3$) for only a finite range of the inward coupling parameter β. By contrast, the antiwaves persist for all β when the chain is sufficiently long. We remark here that the notion of short can be influenced by the degree of coupling in the chain; this observation is relevant to the application discussed in §6.1, since the local and global coupling is believed to be to multiple oscillators.

To make this more specific, we consider a chain of 18 oscillators, coupled as in §2. Such a chain is long enough that antiwaves persist stably for all values of β. We now increase the extent of the coupling by allowing local interactions between an oscillator and each of its three nearest neighbors to each side. (The local coupling is sinusoidal, as in §2.) Similarly, each of the three end oscillators send long inhibitory connections to the oscillators at a distance of ± 9 away with coupling strength β, and the oscillators 7, 8, and 9 (respectively, 10, 11, and 12) send inhibitory connections outward to oscillator 18 (respectively, 1) with strength γ. Note that, if this chain of length 18 is grouped by threes, the result is analogous to a chain of length 6 (i.e., $m = 3$), with the overlap topology of §2.

Numerical simulations show that the modified chain of length 18 does indeed behave like a chain of length 6: As β is increased with $\gamma = 0$, the antiwaves cease to exist as one of the phase lags increases to about $\pi/2$; this happens for $\beta < 3$.

The above simulations show that the effective length scale is a combination of the length N of the chain and the degree of coupling. We conjecture that, if q denotes the number of oscillators directly affected by a given oscillator (in each of the local and global couplings), then the effective length scale is given by N/q. Indeed, if we fix q and let $N \to \infty$, the behavior is that of a singular two-point boundary value problem. However, if N/q is fixed and $N \to \infty$, the behavior is that of an integral equation. (See [24].)

REFERENCES

[1] A. H. COHEN, G. B. ERMENTROUT, T. KIEMEL, N. KOPELL, K. A. SIGVARDT, AND T. WILLIAMS, *Modelling of intersegmental coordination in the lamprey central pattern generator for locomotion*, Trends in the Neurosciences, 15 (1992), pp. 434–438.

[2] S. GRILLNER AND S. KASHIN, *On the generation and performance of swimming in fish*, in Neural Control of Locomotion, R. M. Herman, S. Grillner, P. S. G. Stein, and D. G. Stuart, eds., Plenum Press, New York, 1976, pp. 181–202.

[3] S. GRILLNER, J. T. BUCHANAN, P. WALLÉN, AND L. BRODIN, *Neural control of locomotion in lower vertebrates: from behavior to ionic mechanisms*, in Neural Control of Rhythmic Movements in Vertebrates, A. H. Cohen, S. Rossignol, and S. Grillner, eds., John Wiley, New York, 1987, pp. 1–33.

[4] P. WALLÉN AND T. WILLIAMS, *Fictive locomotion in the lamprey spinal cord in vitro compared with swimming in the intact and spinal animal*, J. Physiol., 347 (1984), *pp.* 225–239.

[5] A. H. COHEN, P. J. HOLMES, AND R. H. RAND, *The nature of the coupling between segmental oscillators of the lamprey spinal generator for locomotion: A mathematical model*, J. Math. Biol., 13 (1982), pp. 345–369.

[6] S. GRILLNER, *Locomotion in vertebrates: central mechanisms and reflex interactions*, Physiol. Rev., 55 (1975), pp. 247–304.

[7] N. KOPELL AND G. B. ERMENTROUT, *Symmetry and phaselocking in chains of weakly coupled oscillators*, Comm. Pure Appl. Math., 39 (1986), pp. 623–660.

[8] N. KOPELL, W. ZHANG, AND G. B. ERMENTROUT, *Multiple coupling in chains of oscillators*, SIAM J. Math. Anal., 21 (1990), pp. 935–953.

[9] G. B. ERMENTROUT AND N. KOPELL, *Multiple pulse interactions and averaging in coupled neural oscillators*, J. Math. Biol., 29 (1991), pp. 195–217.

[10] N. KOPELL, G. B. ERMENTROUT, AND T. WILLIAMS, *On chains of oscillators forced at one end*, SIAM J. Appl. Math., 51 (1991), pp. 1397–1417.

[11] K. A. SIGVARDT, N. KOPELL, G. B. ERMENTROUT, AND M. P. REMLER, *Effects of local oscillator frequency on intersegmental coordination in the lamprey locomotor* CPG: *Theory and experiment*, Soc. Neuroscience Abstracts, 17 (1991), p. 122.

[12] C. ROVAINEN, *Effects of groups of propriospinal interneurons on fictive swimming in the isolated spinal cord of the lamprey*, J. Neurophysiol., 54 (1985), *pp.* 959–977.

[13] A. H. COHEN, *The Structure and function of the intersegmental coordination system in the lamprey spinal cord*, J. Comp. Physiol., 160 (1987), pp. 181–193.

[14] T. KIEMEL, *Three Problems from the Mathematics of Neural Oscillations*, Ph.D. thesis, Cornell University, Ithaca, NY, 1989.

[15] N. KOPELL AND G. B. ERMENTROUT, *Phase transitions and other phenomena in chains of oscillators*, SIAM J. Appl. Math., 50 (1990), pp. 1014–1052.

[16] G. B. ERMENTROUT AND N. KOPELL, *Frequency plateaus in a chain of weakly coupled oscillators*, I, SIAM J. Math. Anal., 15 (1984), pp. 215–237.

[17] N. KOPELL, *Toward a theory of modelling central pattern generators*, in Neural Control of Rhythmic Movements, A. Cohen, S. Grillner, and S. Rossignol, eds., John Wiley, New York, 1987, pp. 369–413.

[18] J. D. MURRAY, *Mathematical Biology*, Springer-Verlag, New York, 1980.

[19] H. MEINHARDT, *Models of Biological Pattern Formation*, Academic Press, New York, 1982.

[20] A. M. TURING, *The chemical basis of morphogenesis*, Phil. Trans. Roy. Soc. B, 237 (1952), pp. 37–72.

[21] G. B. ERMENTROUT, *The behavior of rings of coupled oscillators*, J. Math. Biol., 23 (1985), *pp.* 55–74.

[22] G. E. COGHILL, *Anatomy and the Problem of Behavior*, Hafner, New York, 1929.

[23] A. BEKOFF, *Development of locomotion in vertebrates: A comparative perspective*, in The Comparative Development of Adaptive Skills: Evolutionary Implications, E. S. Gallin, ed., L. Erlbaum Assoc., Hillsdale, NJ, 1985, pp. 57–94.

[24] G. B. ERMENTROUT, *Stable periodic solutions to discrete and continuum arrays of weakly coupled nonlinear oscillators*, SIAM J. Appl. Math., 52 (1992), pp. 1665–1687.

[25] D. H. SATTINGER, Group Theoretic Methods in Bifurcation Theory, Springer Lecture Notes in Mathematics, 762, Springer-Verlag, Berlin, 1979.

[26] N. KOPELL AND D. SOMERS, manuscript in preparation

[27] G. B. ERMENTROUT AND N. KOPELL, unpublished material.

[28] T. L. WILLIAMS, S. GRILLNER, V. SMOLJANINOV, P. WALLÉN, S. KASHIN, AND S. ROSSIGNOL, *Locomotion in lamprey and trout: the relative timing of activation and movement*, J. Exp. Biol., 143 (1989), 559–566.

[29] E. J. FURSHPAN AND D. D. POTTER, *Low resistance junctions between cells in embryos and tissue cultures*, in Current Topics in Developmental Biology, A. Moscona and A. Monroy, eds., Academic Press, New York, 1968, pp. 95–127.

[30] R. L. TRELSTED, J. P. REVEL, AND E. D. HAY, *Tight junctions between cells in the early chick embryo as visualized with the electric microscope*, J. Cell Biol., 31 (1966), pp. C6–C10.

[31] G. B. ERMENTROUT AND N. KOPELL, *Learning of phase-lags in coupled neural oscillators*, Nèural Comput., in press.

[32] H. W. LISSMAN, *Locomotory adaptations and the problem of electric fish*, in The Cell and the Organism, J. A. Ramsey and V. B. Wigglesworth, eds., Cambridge University Press, Cambridge, UK, 1961, pp. 301–317.

[33] A. H. COHEN, *Evolution of the vertebrate central pattern generator for locomotion*, in Neural Control of Rhythmic Movements, A. Cohen, S. Grillner, and S. Rossignol, eds., John Wiley, New York, 1987, pp. 129–166.